University of Southern Queensland

Faculty of Health, Engineering & Sciences

Axisymmetric Scramjet Inlet Operation With Varying Cowl Positions

A dissertation submitted by

Mitchell Kerr

in fulfilment of the requirements of

ENG4112 Research Project

towards the degree of

Bachelor of Engineering (Mechanical)

Submitted: October, 2013

Abstract

The starting behaviour of scramjet inlets is a widely researched area as scramjets have the potential to reduce the cost and improve efficiencies in applications where rockets are traditionally used. The main advantages of scramjet engines are; they have no moving parts, they do not need to carry oxidizers and they are capable of flying at very high speeds.

This project analyses the starting behaviour of a typical axisymmetric scramjet inlet. The inlet consists of a conical forebody with a half angle of 12.28 degrees and a typical axisymmetric cowl. The inlet was tested in the TUSQ hypersonic wind tunnel facility located at the University of Southern Queensland, Toowoomba, Queensland. The inlet was analyzed under both static cowl conditions and dynamic cowl conditons.

To be able to test the inlet a mechanical means of guiding and actuating the cowl was first designed and developed. The design is based on a simple piston and bore concept where pressuised air is used to accelerate the cowl forwards. Once the guidance and actuation system was manufactured it was apparent that some aspects of the system were flawed which meant not all conclusions drawn could be completely validated. The flaw in the system is that the cowl leading edge has a total movement of approximately 1.7 mm in the vertical direction. This movement meant that the results from the static cowl tests are merely estimates and cannot be taken as exact. The results of the dynamic cowl condition are still valid because the main objective of the dynamic test is to investigate if the actuation of the cowl differs the results from the static tests.

The final static results indicate that the Kantrowitz limit is a very good estimate of where the inlet can self start, while the dynamic test results indicate that it is possible to change the inlet starting behaviour by implementing and actuating cowl.

University of Southern Queensland

Faculty of Engineering and Surveying

ENG4111/2 *Research Project*

Limitations of Use

The Council of the University of Southern Queensland, its Faculty of Health, Engineering & Sciences, and the staff of the University of Southern Queensland, do not accept any responsibility for the truth, accuracy or completeness of material contained within or associated with this dissertation.

Persons using all or any part of this material do so at their own risk, and not at the risk of the Council of the University of Southern Queensland, its Faculty of Health, Engineering & Sciences or the staff of the University of Southern Queensland.

This dissertation reports an educational exercise and has no purpose or validity beyond this exercise. The sole purpose of the course pair entitled "Research Project" is to contribute to the overall education within the student's chosen degree program. This document, the associated hardware, software, drawings, and other material set out in the associated appendices should not be used for any other purpose: if they are so used, it is entirely at the risk of the user.

Dean

Faculty of Health, Engineering & Sciences

Certification of Dissertation

I certify that the ideas, designs and experimental work, results, analyses and conclusions set out in this dissertation are entirely my own effort, except where otherwise indicated and acknowledged.

I further certify that the work is original and has not been previously submitted for assessment in any other course or institution, except where specifically stated.

Mitchell Kerr

0061002846

Signature

Date

Acknowledgments

I would like to extend thanks to my supervisor, David Buttsworth, for his expert guidance and support throughout this project.

I was also like to thank Ray Malpress and Paul Baker for their assistance throughout the year. In particular Ray for his guidance and advice and Paul for assisting me with the operation of the tunnel.

Finally I would like to thank my finance, Miss Sarah Sipple, for her support and patience throughout the year.

MITCHELL KERR

University of Southern Queensland

October 2013

Contents

Abstract **i**

Acknowledgments **iv**

List of Figures **ix**

List of Tables **xii**

Nomenclature **xiii**

Chapter 1 Introduction **1**

1.1 Project Background 1

1.2 Project Aim and Objectives 5

1.3 Justification 6

1.4 Conclusion 6

Chapter 2 Literature Review **7**

2.1 Introduction 7

2.2 Scramjets 7

2.2.1 Hypersonic Flow 7

2.2.2 How a Scramjet Works 8

2.3 Scramjet Inlets 10

2.3.1 Inlet Starting and Unstarting 11

2.3.2 Effect of Cowl Positioning 12

2.3.3 Inlet Performance 13

2.4 Risk Management 14

2.4.1 Introduction 14

2.4.2 Risk Identification 14

2.4.3 Risk Evaluation and Control 15

2.5 Conclusion 16

Chapter 3 Design of Guidance and Actuation System 18

3.1 Introduction 18

3.2 Pre-Existing Parts 18

3.2.1 Cowl 19

3.2.2 Inlet 20

3.2.3 Setup 21

3.3 Initial Concepts 21

3.3.1 Guidance and Mounting System 21

3.3.2 Actuation System 26

3.4 Design Choice 29

3.4.1 Guidance and Mounting System 29

3.4.2 Actuation System 30

3.5 Component Design 32

3.5.1 Actuation Force Requirements 33

3.5.2 Sealing of Design 34

3.6 Final Design 35

Chapter 4 Experiment Design **38**

4.1 Testing Environment and Equipment 38

4.2 Required Data 39

4.3 Kantrowitz Limit 40

4.4 Cowl Testing Positions 42

Chapter 5 Results and Discussion **45**

5.1 Introduction 45

5.2 Flow Conditions 45

5.3 Inconsistencies in Results 46

5.4 Static Tests 49

5.5 Dynamic Test 50

Chapter 6 Conclusions **55**

6.1 Limitations 55

6.2 Static Tests 56

6.3 Dynamic Tests 56

6.4 Further Work 56

6.5 Conclusion 57

References **58**

Appendix A Project Specification **62**

Appendix B Manufacturing Drawings **64**

Appendix C Matlab Code **72**

C.1 The `kantrowitzlimit.m` MATLAB Script 73

C.2 The `MachNo.m` MATLAB Script 75

Appendix D Pressure Results **76**

List of Figures

1.1 Scramjet schematic (FIS 2007) 2

1.2 Artist's illustration of the X43-A vehicle (NASA 2004) 3

1.3 Propulsion performance of different types of aircraft (FighterPlanes.com 2000) 5

2.1 Shock waves in and around a scramjet (NASA 2009*a*) 8

2.2 Comparison of hydrocarbon fuels against hydrogen fuels (Fry 2004) . . . 9

2.3 External compression inlet (Heiser 1994) 10

2.4 mixed compression inlet (Heiser 1994) 10

2.5 internal compression inlet (Heiser 1994) 10

2.6 Axisymmetric inlet stations (Curran 2000) 11

2.7 Boundary layer seperation (Curran 2000, 462) 12

2.8 Schliern flow visualisation showing an unstarted inlet (Left) and a started inlet (Right) (NASA 2009*b*) 13

2.9 A typical Schlieren flow visulisation setup (NASA 2009*c*) 14

3.1 Inlet assembly concept derived by Harrland (2012) 19

3.2 Axial locations of pressure transducers 20

3.3 Sketch of Concept 1 22

3.4 Picture of Concept 2 23

3.5 Sketch of Concept 3 24

3.6 Sketch of Concept 4 25

3.7 Exploded drawing of final design 35

4.1 Schematic of TUSQ hypersonic facility (Buttsworth 2009) 38

4.2 Schlieren flow visulisation setup 39

4.3 Unfiltered data (left) compared to filtered data (right) (run 265 shown) 40

4.4 Barrel pressure history (run 264 shown) 41

4.5 Flow chart representing Kantrowitz limit calculation 42

4.6 Sketch of the Inlet Compression Geometry 43

4.7 Inlet and Cowl Matlab Model 43

4.8 Physical location of zero position 44

5.1 Flow visulisation of runs 267 (left) and 265 (right) taken 100 ms after the start of the flow 50

5.2 Pressure measurements of runs 267 (left) and 265 (right) 50

5.3 Comparison of run 268 and run 271 at the same position 51

5.4 Comparison of run 269 and run 271 at the same position 52

5.5 Flow visulisation of run 266 53

5.6 Surface pressure measurements of run 271 53

5.7 1 ms before the end of actuation (top) followed by three images taken 1 ms apart after collision with stopper 54

List of Tables

1.1 Scramjet evolution 1955-1990 (Fry 2004) 3

1.2 Scramjet evolution 1990-2003 (Fry 2004) 3

2.1 Risk assessment matrix 15

2.2 Risk assessment 17

3.1 Guidance and mounting system concept weighting 30

3.2 Guidance and mounting system concept decision matrix 30

3.3 Actuation system concept weighting 31

3.4 Actuation System Concept Decision Matrix 31

3.5 Limitations of design 32

3.6 O–Ring specifications (StandardsAustralia 1986) 34

4.1 Location of the cowl for each run 43

5.1 Operating conditions of each run 46

5.2 Flow Conditions 47

5.3 Summary of static cowl runs 49

Nomenclature

A	Area
M	Mach number
γ	Ratio of specific heats
S	Position
v	Velocity
t	Time
a	Acceleration
P	Pressure
c	Speed of sound
R	Specific gas constant
G	Modulus of rigidity
T	Temperature
F	Force
F_f	Frictional force
L	Length
m	Mass
d	Distance
r	Radius
ϕ	Angle of Twist

Chapter 1

Introduction

This chapter describes the project outline and objectives. The primary purpose of this project is to investigate an axisymmetric scramjet inlet operation with varying cowl positions.

1.1 Project Background

There has always been the need for people to create faster and more efficient modes of travel and recently people have been investigating the possibility of scramjet technology. Scramjet stands for 'supersonic combustion ramjet' and can be defined as 'a ramjet airplane engine in which thrust is produced by burning fuel in a supersonic air stream after the airplane has attained supersonic speed by other means of propulsion'(Merriam-Webster 2010).

As you can see in Figure 1.1, there are three sections to a typical scramjet engine. The first section is the intake, this is where hypersonic air flow is captured and compressed by the intake geometry. The second section is the combustion section where fuel is injected into the airflow and ignited. Section three is the diverging nozzle where the expanding air is accelerated to produce thrust.

The main advantages of scramjet engines are:

- They have absolutely no moving parts

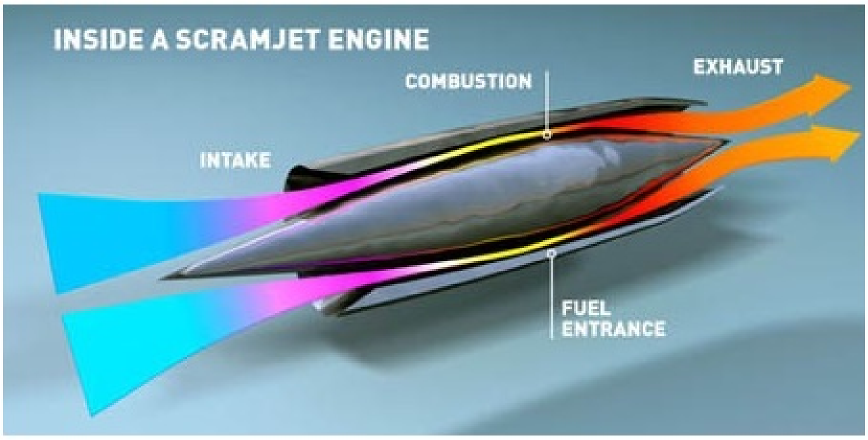

Figure 1.1: Scramjet schematic (FIS 2007)

- They don't need to carry oxygen (like rockets)
- The high speeds in which they are capable of traveling.

The disadvantages of scramjet engines are:

- They need to be brought to hypersonic speeds by another method before they start working.
- The harsh conditions associated with high speeds (large drag forces and very hot conditions)

The development of the scramjet engine started in the mid 1950s through early 1960s when it was realised that it is too inefficient to slow down the airflow to subsonic speeds within a ramjet at high Mach numbers (Roberts 2008). After the benefits of scramjet technology were realised, the first scramjet demonstration was completed by Ferri in 1960 (Fry 2004). Soon after Ferri many scramjet development programs started to appear around the world. The most notable of these was the Hypersonic Ramjet Experiment or Hypersonic research Experiment (HRE) which was started in May 1964 (Heiser 1994). The main aim of this program was to 'test a complete, regeneratively cooled, flight weight scramjet on the X-15A-2 rocket research airplane' (Heiser 1994). This program was terminated in 1968 because the test vehicle was damaged in a flight and was seen as too costly to repair. There have been many more programs since and they can be seen compiled in Table 1.1 and Table 1.2 (Fry 2004).

Table 1.1: Scramjet evolution 1955-1990 (Fry 2004)

Era	Country/service	Engine/vehicle	Engine type	Dates, year	Cruise Mach no.	Cruise altitude, ft	Powered range, n mile	Launcher	Total length, in.	Diameter, in.	Total weight, lbm	State of development
1955–1975	U.S. Navy	External burn[b]	ERJ	1957–1962	5–7	—	—	—	—	—	—	Combustion tests
	Russia	Chetinkov research	ERJ	1957–1960	5–7	—	—	—	—	—	—	Component tests
	U.S. Air Force	Marquardt SJ	DMSJ	1960–1970	3–5	—	—	—	88	10 × 15	—	Cooled engine tests
	U.S. Air Force	GASL SJ[a]	SJ	1961–1968	3–12	—	—	—	40	31 in^2	—	Cooled engine tests
	U.S. Navy	SCRAM[b]	LFSJ	1962–1977	7.5	100,000	350	Rail	288	26.2	5,470	Free-jet test
	U.S. Air Force	IFTV[c]	H_2/SJ	1965–1967	5–6	56,000	—	—	—	—	—	Component tests
	U.S. Air Force–NASA	HRE[a]	H_2/SJ	1966–1974	4–7	—	—	—	87	18	—	Flowpath tests
	NASA	AIM[b]	H_2/SJ	1970–1984	4–7	—	—	—	87	18	—	Cooled engine tests
	France	ESOPE[b]	DMSJ	1973–1974	5–7	—	—	—	87	18	—	Component tests
1975–1990	U.S. Navy	WADM/HyWADM[b]	DCR	1977–1986	4–6	80,000–100,000	500–900	VLS	256	21	3,750	Component tests
	Russia	Various research	SJ/DCR	1980–1991	5–7	80,000–100,000	—	—	—	—	—	Combustion tests
	NASA	NASP[b]	MCSJ	1986–1994	0–26	0–orbit	Orbital	Runway	—	—	500,000	Free-jet test (M7)
	Germany	Sänger II[b]	ATRJ	1988–1994	4	0–orbit	Orbital	Runway	3976	550	800,000	Concept vehicle

[a]System discussed and shown. [b]System discussed. [c]IFTV incremental flight test vehicle.

Table 1.2: Scramjet evolution 1990-2003 (Fry 2004)

Era	Country/service	Engine/vehicle	Engine type	Dates, year	Cruise Mach no.	Cruise altitude, ft	Powered range, n mile	Launcher	Total length, in.	Diameter, in.	Total weight, lbm	State of development
1990–2003	United Kingdom	HOTOL[c]	SJ	1990–1994	2–8	—	—	—	—	—	—	Combustion tests
	Japan	PATRES/ATREX[b]	TRBCC	1990–	0–12	100,000	—	—	87	30	—	Component tests
	Japan	NAL-KPL research[b]	SJ	1991–	4–12	50,000–100,000	—	—	83	8 × 10	—	Component tests
	Russia	Kholod[a]	DCR	1991–1998	3.5–5.4	50,000–115,000	—	SA-5	36	24	—	Flight tests
	Russia/France	Kholod[a]	DCR	1991–1995	3.5–5.4	50,000–115,000	—	SA-5	36	24	—	Flight tests
	Russia/United States	Kholod[a]	DCR	1994–1998	3.5–7	50,000–115,000	—	SA-5	36	24	—	Flight tests
	France	CHAMIOS[b]	SJ	1992–2000	6.5	—	—	—	—	8 × 10	—	Component tests
	France	Monomat	DMSJ	1992–2000	4–7.5	—	—	—	—	4 × 4	—	Component tests
	France	PREPA[a]	DMSJ	1992–1999	2–12	0–130,000	Orbital	Ground	2560	Waverider	1 × 10^6	Component tests
	Russia	ORYOL/MIKAKS	SJ	1993–	0–12	0–130,000	Orbital	Ground	—	—	—	Component tests
	France/Russia	WRR[b]	DMSJ	1993–	3–12	0–130,000	—	Ground	—	Waverider	60,000	Component tests
	Russia	GELA Phase II[a]	RJ/SJ	1995–	3–5+	295,000	—	Tu-22M	—	—	—	Flight tests
	Russia	AJAX[b]	SJ	1995–	0–12	0–130,000	—	—	—	—	—	Concept
	U.S. Air Force	HyTech[a]	SJ	1995–	7–10	50,000–130,000	—	—	87	9 × 12	—	Component tests
	United States	GTX[d]	RBCC[e]	1995–	0–14	50,000–130,000	—	—	—	—	—	Component tests
	U.S. Navy	Counterforce	DCR	1995–	4–8	80,000–100,000	—	Air/VLS	256	21	3,750	Component tests
	NASA	X-43A/Hyper-X[a]	H2/SJ	1995–	7–10	100,000	200	Pegasus	148	60(span)	3,000	Flight tests
	France/Germany	JAPHAR[a]	DMSJ	1997–2002	5–7.6	80,000	—	—	90	4 × 4	—	Component tests
	United States	ARRMD[b]	DCR	1997–2001	3–8	80,000	450–800	Rail/Air	168–256	21	2,200–3,770	Component tests
	Russia	IGLA[a]	SJ	1999–	5–14	82,000–164,000	—	SS-25	197	—	—	Flight tests
	NASA	X-43C[b]	DMSJ	1999–	5–7	100,000	—	Pegasus	—	10.5 wide	—	Component tests
	Unites States	IHPTET[b]	ATR	1999–	0–5	0–90,000	—	—	—	15–40	—	Component tests
	United States	RTA[b]	TBCC	1999–	0–5	0–90,000	—	—	—	15–40	—	Component tests
	France	Promethee[b]	DMSJ	1999–2002	2–8	0–130,000	—	—	238	—	3,400	Component tests
	India	AVATAR-M[b]	SJ	1999–	0–14	0–orbit	Orbital	Ground	—	—	18–25 ton	Combustion tests
	United Kingdom	HOTOL Phase II	SJ	2000–	2–8	—	—	—	—	—	—	Component tests
	France	PIAF[b]	DMSJ	2000–	2–8	0–110,000	—	—	53	8 × 2	—	Component tests
	United States	MARIAH	MHD/SJ	2001–	15	—	—	—	—	—	—	Combustion tests
	Australia	HyShot[b]	SJ	2001–2002	7.6	75,000–120,000	200	Terrior Orion	55	14	—	Flight tests
	United States	Gun launch technology	SJ	2001–	—	—	—	Ground	—	—	—	Flight tests
	United States	ISTAR[b]	RBCC[e]	2002–2003	2.4–7	0-orbit	Orbital	Ground	400	Waverider	20,000	Component tests
	United States	X-43B[b]	RB/TBCC	2002–2003	0–10	100,000	200	Air	500	Waverider	24,000	Component tests
	Russia	Mig-31 HFL[b]	SJ/DCR	2002–	2–10	50,000–130,000	—	Mig-31	—	—	—	Planned flight tests
	United States	HyFly[a]	DCR	2002–	3–6.5	85,000–95000	600	F-4	225	19	2,360	Flight tests planned
	United States	SED[a]	SJ	2003–	4.5–7	80,000	—	—	—	9 wide	—	Planned flight tests
	France	LEA[a]	SJ/DCR	2003–2012	4–8	80,000	—	Air	—	—	—	Flight tests planned
	United States	RCCFD[b]	TBCC	2003–	0.7–7	0–orbit	Orbital	Ground	400	Waverider	20,000	Flight tests planned

[a]System discussed and shown. [b]System discussed. [c]Horizontal takeoff and landing (HOTOL). [d]NASA Glenn Rc hydrogen fueled/cooled (GTX). [e]Reference vehicle designation (RBCC).

Figure 1.2: Artist's illustration of the X43-A vehicle (NASA 2004)

The first ever successful ignition of a scramjet in flight was conducted in the HyShot program conducted by the University of Queensland in 2002 (CenterForHypersonics 2002). The 15 seconds of ignition validated all the data collected in the ground tests and crossed a hurdle towards the validity of hypersonic aircraft (Catalyst 2002). Shortly after the range of Table 1.2 NASA conducted record breaking tests within their Hyper X program. The 8 year $230 million program had three launches, two of which were successful. There were three X43-A vehicles built during the program, the first two designed for Mach 7 and the third designed for Mach 10. All vehicles were launched used a B-52B aircraft and further accelerated to hypersonic speeds using modified Pegasus rockets. The first test, which was unsuccessful, failed shortly after the rocket was released when the rocket flew out of control. The second test was successful and broke the world speed record for an air breathing vehicle in March 2004 with a speed of Mach 6.8. This record was again broken in November the same year by the third X43-A vehicle which reached a speed of Mach 9.6 (NASA 2009*a*). An artist's illustration of the X43-A vehicles can be seen in Figure 1.2

More recently the United States Air Force has conducted successful scramjet tests. On the 1st of May 2013 they successfully completed the last of its four test flights with its X-51A Waverider vehicle. The Waverider burnt up all of its four minute fuel supply and reached a top speed of Mach 5.1 before crashing into the Pacific Ocean (Wall 2013).

Scramjets are of interest to scientists and engineers worldwide because of the potential to travel at such high speeds without having to carry oxygen or other oxidizers like rockets. The performance of different types of propulsion in regards to operating speeds can be seen in Figure 1.3, which clearly shows the potential of a scramjet propelled vehicle. The main areas of focus at the present time are validating the implementation of scramjet technology into missiles and space launching vehicles. One of the main objectives of the X51-A missions is to develop technology that could lead to a prompt global strike missile that could hit a target anywhere on Earth within an hour (Covault 2010).

The reason scramjets are of interest when it comes to launching objects or vehicles into space is that it is a much cheaper and more efficient way opposed to rockets. Most of a rockets weight is the weight of the oxygen and fuel. Because scramjets are air breathing vehicles there is no need to carry oxygen which also means less fuel will be needed to overcome the extra weight of oxygen.

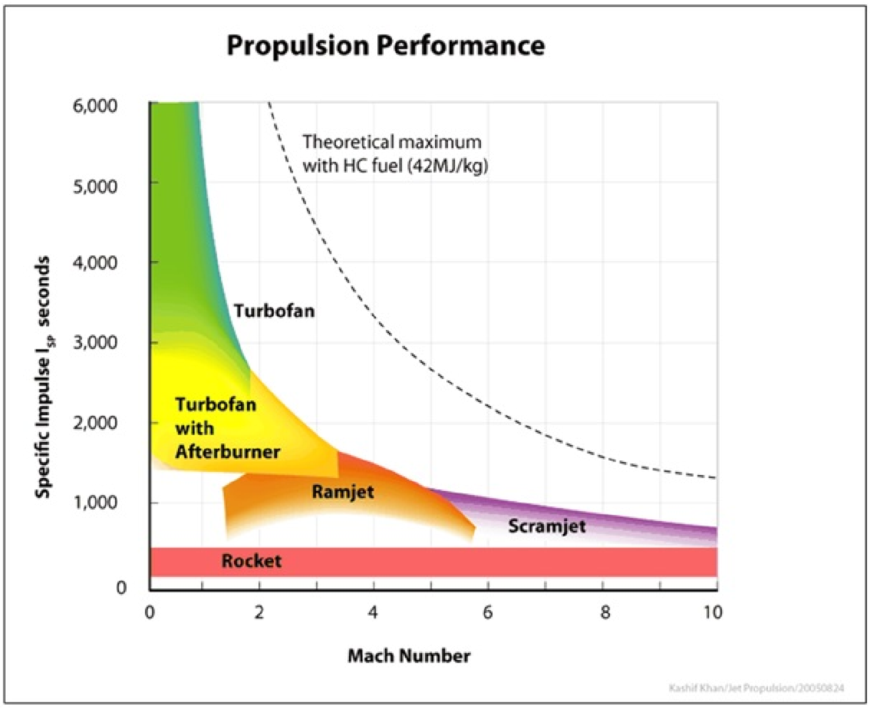

Figure 1.3: Propulsion performance of different types of aircraft (FighterPlanes.com 2000)

1.2 Project Aim and Objectives

This project aims to investigate the operation of an axi-symmetric scramjet inlet with varying axial positions of the cowl. To achieve this aim the project needs to be broken down into individual objectives. These are:

- Research the background information that relates to axisymmetric scramjet design and cowl positioning.
- Research methods that can be used to quantify the performance of the inlet
- Design and develop a method of positioning and actuating the cowl
- Improve the mounting of the existing pressure transducers so that they don't affect the airflow
- Design an experiment to evaluate the performance of the inlet at the different cowl positions
- Analyse the performance of the inlet in the hypersonic wind tunnel at the University of Southern Queensland (USQ)
- Assess the experimental results of the inlet at the different cowl positions

1.3 Justification

The increasing need to develop faster and more efficient technology means it is inevitable that the possibility of scramjet technology is investigated. This project will make it possible to classify the behaviour of the inlet at different cowl positions and it will also analyse the effects of a dynamic cowl condition. This will allow this scramjet inlet to be more efficient and allow the potential benefits of an actuating cowl to be realised.

1.4 Conclusion

This project aims to investigate the performance of an axi-symmetric scramjet inlet with varying cowl positions. A literature review will be conducted to determine the previous progress and the constraints and limitations of this type of project. After the initial research is complete a method of actuating the cowl will be designed and implemented so that the different conditions can be tested in the hypersonic wind tunnel at USQ. After the experimentation stage the results will be used to assess the overall performance of the inlet.

Chapter 2

Literature Review

2.1 Introduction

This chapter will review and analyse the current literature and publications regarding scramjet inlet operations.

2.2 Scramjets

To fully gain an understanding of the parameters and limitations of this project, relevant literature must be reviewed on scramjets themselves. This section will investigate literature relating to; hypersonic flow, how a scramjet works and scramjet inlets.

2.2.1 Hypersonic Flow

To fully understand a scramjet there must be a brief understanding of hypersonic flow. Pritchard (2011) defines supersonic flow as flow greater than Mach 1 and hypersonic flow as flow equal to or greater that Mach 5. Once supersonic flow is reached shock waves are formed. When an object reaches the speed of sound it catches up to the pressure waves caused by the object traveling through the air (HowThingsFly 2012). This means that the air in front of the object has no warning something is coming and doesn't start flowing out of the way. This causes the object to 'plough' through the air creating the

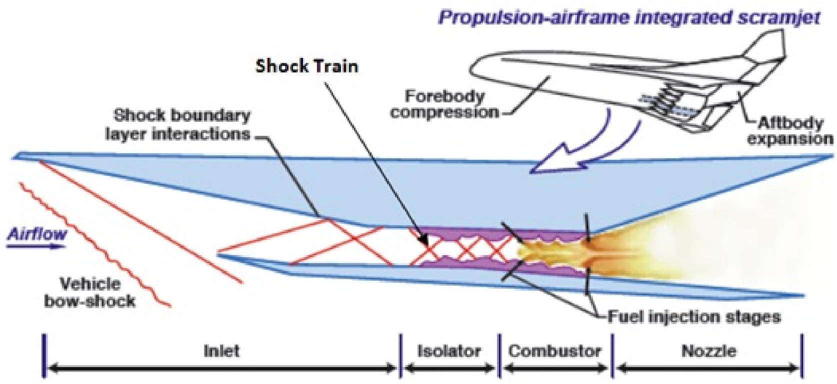

Figure 2.1: Shock waves in and around a scramjet (NASA 2009*a*)

shock wave (HowThingsFly 2012) . Further to this the AernauticalHandbook (2009) goes on to say that when air passes through the shock wave it is forced to suddenly make drastic changes in pressure, density, temperature and velocity.

These changes due to the shock waves both hinder and help with the design of a scramjet. Before the air reaches the combustor it must be slowed down to some degree and this is accomplished by the formation of a 'shock train' upstream of the fuel injection (Smart 2003*b*), seen in Figure 2.1.

A way in which the shock waves hinder the performance of a scramjet is the fact that there is such a sudden and harsh change in conditions. Finding ways of cooling the scramjet and finding materials that can cope with the high temperatures is another area of research all on its own.

For a fluid flow to be steady and predictable the boundary layer must not separate (Pritchard 2011). Fielding (2007) explains this further saying 'once separation has occurred the flow behind the separation point typically comprises of a vortex filled wake that differs drastically from the predictions of inviscid theory'. In essence, if the flow is steady and uniform the pressure along the contacting surface must be uniform.

2.2.2 How a Scramjet Works

In section 1.1 the general working of a scramjet was briefly described. This section will go into how they work in more detail. As mentioned earlier there are three main stages within a scramjet:

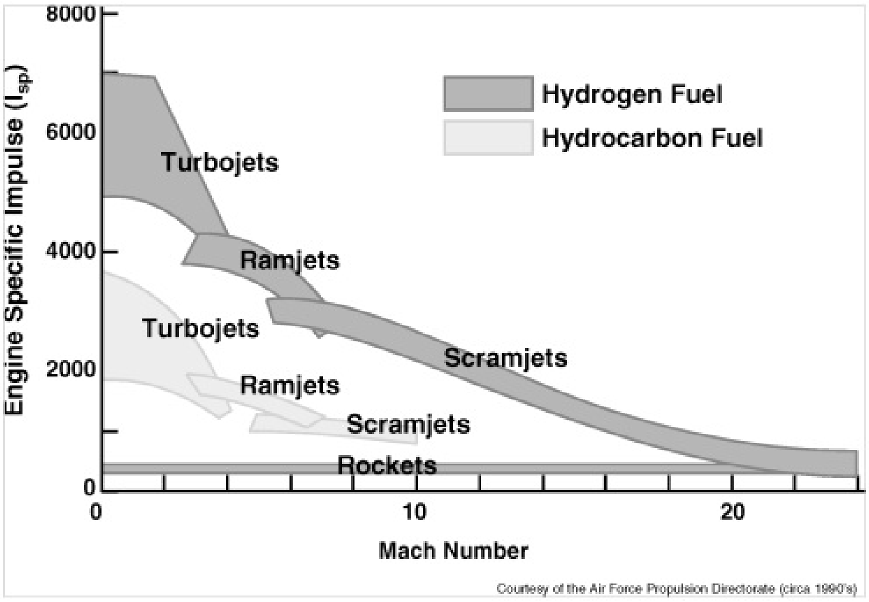

Figure 2.2: Comparison of hydrocarbon fuels against hydrogen fuels (Fry 2004)

- Intake
- Combustion
- Exhaust

The purpose of the inlet is to capture and compress air so that it can be processed by the rest of the engine. This compression occurs when the air passes through the shock waves caused by the geometry of the inlet (Andreadis 2004). After the air is initially compressed the air flows to the combustion section of the engine.

In this section of the scramjet fuel is injected in stages so that a uniform mix of fuel and air can be achieved before combustion occurs (Roberts 2008). The two types of fuel that are used in scramjet engines are hydrocarbon fuels and hydrogen (ADFA 2007). The comparison of the two fuels can be seen in Figure 2.2.

After the combustion stage the hot exhaust gases pass through a nozzle that causes the air to expand and accelerate which in turn creates thrust (NASA 2008).

2.3 Scramjet Inlets

Hypersonic inlets used in scramjets fall into three different categories; external compression, mixed compression and internal compression (Smart 2003*a*). As the names suggest these categories are determined by the way in which the air is compressed. These three different types of inlets can be seen in Figure 2.3, Figure 2.4 and Figure 2.5.

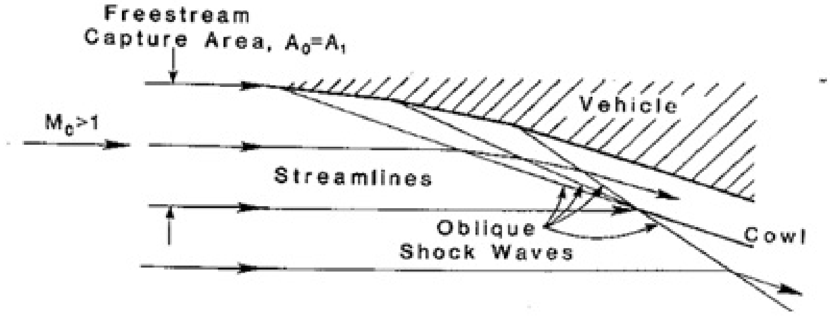

Figure 2.3: External compression inlet (Heiser 1994)

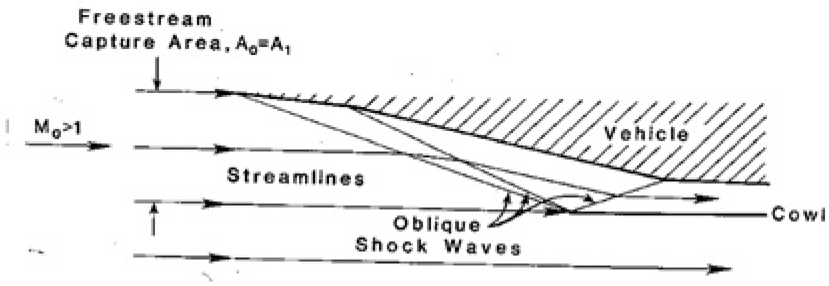

Figure 2.4: mixed compression inlet (Heiser 1994)

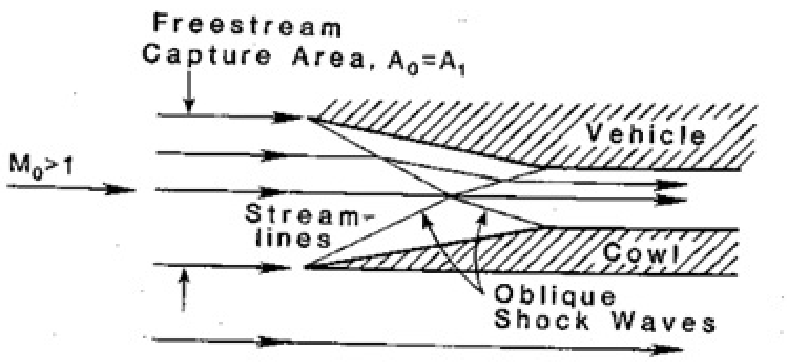

Figure 2.5: internal compression inlet (Heiser 1994)

It was found through a range of experiments that for an inlet to function well in a range of Mach numbers the best choice is to use a mixed compression inlet (Smart 2003*a*). The inlet investigated during this project is a mixed compression inlet. Figure 2.6 defines the different stations of an axisymmetric inlet similar to the one used in this

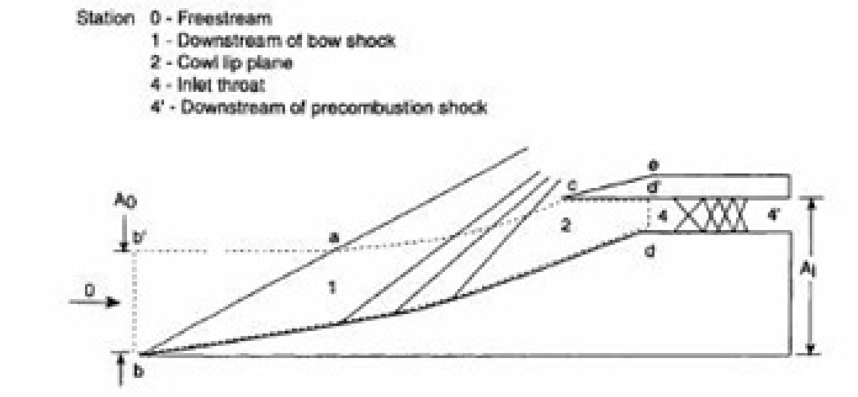

Figure 2.6: Axisymmetric inlet stations (Curran 2000)

project.

2.3.1 Inlet Starting and Unstarting

Inlet starting and unstarting is the most commonly researched behaviour of hypersonic inlets. Figure 2.9 shows the visual difference between a started inlet and an unstarted one. Unstarting of an inlet occurs when the capture mass flow rate does not equal the downstream mass flow rate of the engine (Prakash 2006). The main reason a scramjet will choke (unstart) is because the flow has been slowed down too much. The flow is slowed down because when an inlet unstarts a normal shock is expelled, which causes flow to be spilled subsonically (Curran 2000). The slowing down of the flow due to the shock waves could be by two ways; the free stream velocity might not be quick enough to ensure the velocity after the shock stays above the limit and the shock system could be strong enough that it causes the boundary layer to separate resulting in a flow field shown in Figure 2.7 (Curran 2000).

Methods than can potentially be used to start an unstarted inlet are (Prakash 2006):

- Overspeeding or increasing the free stream Mach number.
- Using variable geometry to change the area ratio

The process of overspeeding refers to the inlet, or free steam, being accelerated to a high enough velocity that the velocity at the capture area is high enough to allow the inlet to start (Prakash 2006). Curran (2000) also mentions that overspeeding can be

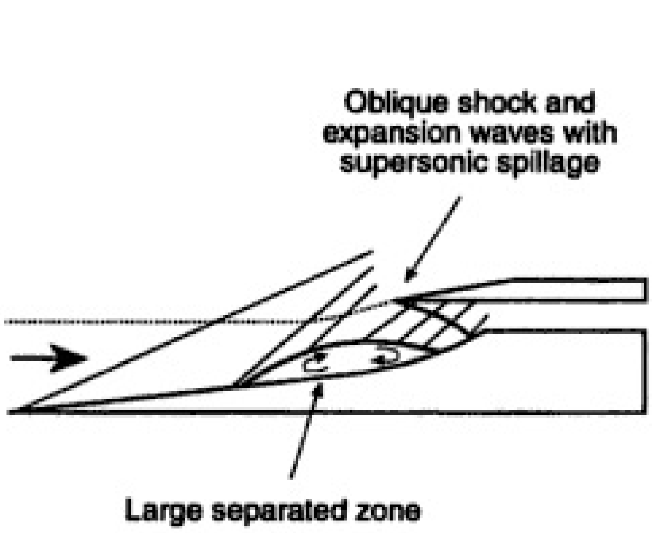

Figure 2.7: Boundary layer seperation (Curran 2000, 462)

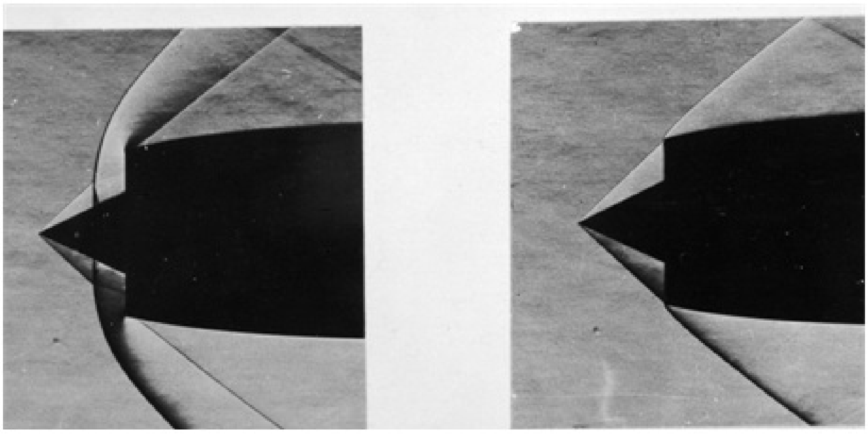

Figure 2.8: Schliern flow visualisation showing an unstarted inlet (Left) and a started inlet (Right) (NASA 2009*b*)

utilised as a method of starting an inlet because during this process the angle of the oblique nose shock changes.

Using variable geometry in scramjets is of high interest to researchers and engineers because the potential for the inlet to operate at a variety of Mach numbers (Mahapatra 2008). The only problem with variable geometry inlets is the mechanical feasibility because the aerodynamic design of this particular type of inlet is quite simple (Mahapatra 2008). Variable geometry inlets allow an inlet to be started and the general performance of the inlet increased because the contraction ratio can be controlled to some degree.

2.3.2 Effect of Cowl Positioning

The main effect the positioning of the cowl will have is whether or not the inlet 'starts'. Inlet starting has been researched quite extensively and its been found that the likelihood of starting is determined by the local Mach number, the internal contraction ratio and the diffuser flow field pressure recovery (Curran 2000). Obtaining an estimate of the contraction ratio that will allow the engine to self start can be done using the Kantrowitz limit. The equation for the Kantrowitz limit is (Curran 2000):

$$\frac{A_2}{A_4}_{Kantrowitz} = \frac{1}{M_2}\left[\frac{(\gamma+1)M_2^2}{(\gamma-1)M_2^2+2}\right]^{\frac{\gamma}{\gamma-1}}\left[\frac{\gamma+1}{2\gamma M_2^2-(\gamma-1)}\right]^{\frac{1}{\gamma-1}}\left[\frac{1+(\frac{\gamma-1}{2})M_2^2}{\frac{(\gamma+1)}{2}}\right]^{\frac{\gamma+1}{2(\gamma-1)}} \tag{2.1}$$

The subscripts 2 and 4 of Equation 2.1 relate to the inlet stations seen in Figure 2.6. The limit is determined by assuming a normal shock at the beginning of the internal contraction and calculating the one-dimensional, isentropic, internal area ratio that will produce sonic flow at the inlet throat (Curran 2000). Curran (2000) and Throckmorton, Schetz & Jacobsen (2010) both describe the Kantrowitz limit as a conservative starting point for the selection of the inlet area. Curran (2000) states 'the reason the Kantrowitz limit is conservative is because of the assumption of a singular normal shock at the cowl lip station' which in reality does not happen.

2.3.3 Inlet Performance

There are many different aspects of a hypersonic inlet that can be measured as an indication of some sort of performance. The literature reviewed for this project will consist solely on ways to measure or determine if the inlet has started or not.

The most common way of determining if an inlet starts or not is by using a form of flow visulisation known as Schlieren flow visulisation. Schlieren flow visulisatioin is a technique which relies on the fact that light gets bent when passing through changes of density in a fluid (NASA 2009*c*). A typical Schlieren setup can be seen in Figure 2.9. Schlieren flow visulisation is ideal for compressible flow because shock waves are easily seen because they cause huge changes in density (Hu 2004).

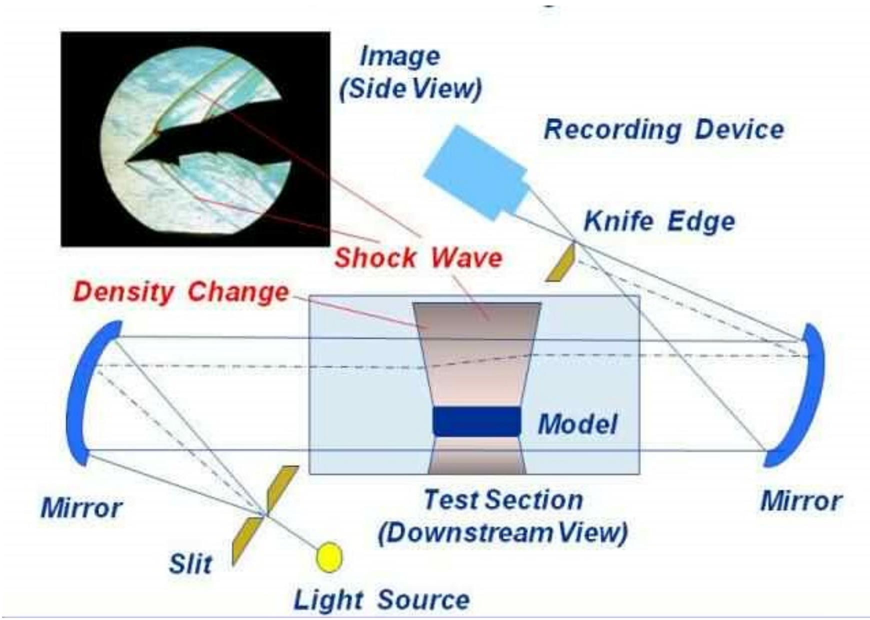

Figure 2.9: A typical Schlieren flow visulisation setup (NASA 2009*c*)

Another common method of determining if a inlet has started or not is by taking pressure measurements. As mentioned in section 2.2.1, for the flow to be uniform and steady (a started inlet) the pressure along the contacting surface must be uniform. Pressure measurements are commonly used by researchers alongside flow visulisation to help explain apparent fluctuations in the boundary layer (Casper 2009).

2.4 Risk Management

2.4.1 Introduction

To safely complete this project a risk assessment must first take place to identify any potential risks or hazards. This risk assessment will examine all possible sources that pose a potential risk and put a plan into place to reduce the likelihood of each risk.

2.4.2 Risk Identification

The possible risks associated with this project are:

- Working around pressurised air

- Moving parts
- Sharp edges and vertices
- Electrical hazards when operating power supply and solenoid
- Burn hazard when operating a soldering iron

2.4.3 Risk Evaluation and Control

The chosen method of evaluating the risks involved with this work is to develop a risk assessment matrix. The risk assessment matrix is then used to determine the necessary steps that need to be taken to eliminate the risk. The use of a risk assessment matrix is the usual industry standard and this will be more than adequate for this particular purpose. The risk assessment matrix used to evaluate the potential risks outlined in section 2.4.2 can be seen in Table 2.1.

Table 2.1: Risk assessment matrix

			Consequences				
			1 – Insignificant Dealt with by in-house first aid, etc	2 – Minor Medical help needed. Treatment by medical professional/hospital outpatient, etc	3 – Moderate Significant non-permanent injury. Overnight hospitalisation (inpatient)	4 – Major Extensive permanent injury (eg loss of finger/s) Extended hospitalisation	5 – Catastrophic Death. Permanent disabling injury (eg blindness, loss of hand/s, quadriplegia)
Likelihood	A	Almost certain to occur in most circumstances	High (H)	High (H)	Extreme (X)	Extreme (X)	Extreme (X)
	B	Likely to occur frequently	Moderate (M)	High (H)	High (H)	Extreme (X)	Extreme (X)
	C	Possible and likely to occur at some time	Low (L)	Moderate(M)	High (H)	Extreme (X)	Extreme (X)
	D	Unlikely to occur but could happen	Low (L)	Low (L)	Moderate(M)	High (H)	Extreme (X)
	E	May occur but only in rare and exceptional circumstances	Low (L)	Low (L)	Moderate (M)	High (H)	High (H)

As you can see the chosen risk assessment matrix combines the likelihood of the event occurring with the potential consequences. Each potential risk will be assessed and placed into the appropriate category shown in Table 2.1. Any risk that falls into a category apart from low will be deemed unacceptable and actions should be taken immediately to reduce the potential risk. The final assessment of each potential risk can be seen in Table 2.2.

2.5 Conclusion

After identifying and analysing the potential risks and hazards involved with the project, table 2.2 clearly shows that all risks have appropriate measures and procedures in place that allows them to be in the low risk category. Therefore no further precautions or measures need to be followed as long as the procedures outlined in 2.2 are adhered to.

Table 2.2: Risk assessment

Activity: Testing of inlet under dynamic cowl conditions in P10 facility		**Completed By:** Mitchell Kerr - 20/08/2013	
Identified Risk	**Current Control Measures**	**Level of Risk**	**Actions Required**
Working around pressurised air Pressurised air could cause particles to be blown into the eyes of the operator and surrounding people. There is also potential for hearing damage when connecting and disconnecting the air hose. (note: No air gun is used)	• Ensure fittings are not pointed at operators face • Gradual release of air when initial bench top testing is taking place • Operator does not leave test piece until the air is fully discharged • Only operated by people who know how the test piece works	D2 – Low Risk	No further actions required
Moving parts Working around moving parts means there is a potential pinching and crushing risk.	• All moving parts are underneath the test piece and are not easily assessable. To make this more so when bench top testing occurs the test piece is kept low relative to the bench • When testing occurs hands and other equipment are kept away from the area at all times • When the test is complete air is disconnected (air is the actuation method) before adjusting parts. • Only operated by people who know how it works	E1 – Low Risk	No further actions required
Sharp edges/ points The scramjet model has many sharp points and edges that could potentially cut the operator	• The point at the tip of the inlet always has a section of rubber hose over it to keep the tip out of the way • Once assembled the sharp leading edge of the two guide plates are almost inaccessible and it almost runs flush with the inlet taking away the potential to slice across it. • Only operated by people who are aware of the edges and know how the test piece works.	D2 – Low Risk	No further actions required
Electrical hazard when operating solenoid and power supply There is the potential of an electric shock when operating the power supply and solenoid	• Make sure power supply, wires and solenoid are kept away from water • Make sure power supply is turned off as soon as test is complete. • Solenoid is powered by 12 V so this is a low voltage application.	E1 - Low Risk	No further actions required
Soldering Risk of burns	• Eye protection warn • Stands used to prevent fingers getting too close to work	D1 – Low Risk	No further action required

Chapter 3

Design of Guidance and Actuation System

3.1 Introduction

To effectively test this inlet under dynamic cowl conditions a method of actuating and guiding the cowl must first be developed. The requirements of this design are:

- Must be able to actuate the cowl quickly and reliably
- Must be able to mount the cowl to the inlet
- Must guide the cowl along the required path
- Must be able to be retrofitted to the existing inlet

3.2 Pre-Existing Parts

This particular inlet assembly has been tested and analysed before so there are some pre-existing parts that can be utilised for the research involved with this project. The inlet that is used in these tests was designed by Mr Alan Harrland from the University of Adelaide. Harrland's concept can be seen in Figure 3.1. As mentioned earlier, the inlet assembly consists of a conical forebody with a typical axisymmetric cowl. For

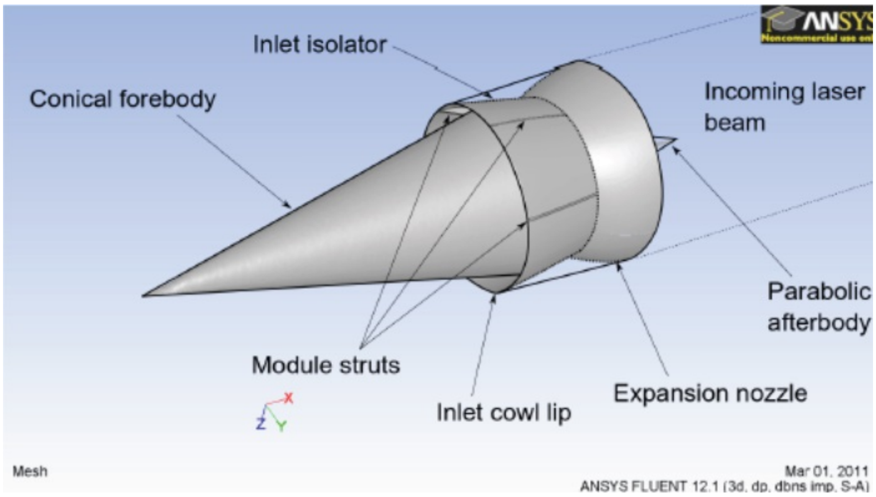

Figure 3.1: Inlet assembly concept derived by Harrland (2012)

testing purposes only 178 degrees of the cowl and rear forebody were manufactured. The inlet designed by Harrland (2012) also included a parabolic afterbody, which for this work the model does not include. The afterbody was needed for Harrland's work with laser propulsion but isn't nessessary for this work.

3.2.1 Cowl

This is obviously utilised for this project as it is one of the two main components that make up the inlet assembly. Issues with the pre-existing cowl that will affect the performance of quality of this project are:

- The method of mounting the cowl to the inlet
- Previous methods of mounting the cowl have left two cut out slots running along the underside of the cowl

To address the problem of mounting the cowl to the inlet a new method of mounting the cowl has been developed and can be seen in section 3.5, when developing the guidance and actuation system. As for the two cut out slots on the underside of the cowl, these were filled with an epoxy filler and smoothed out so there is no disturbance to the flow.

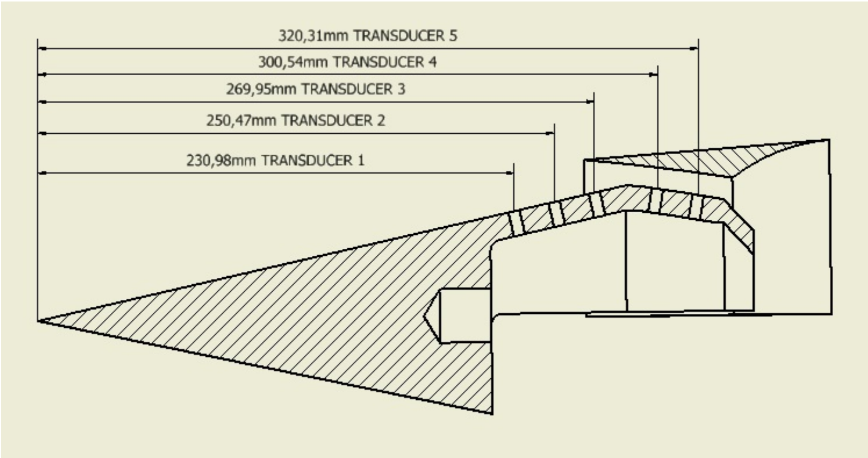

Figure 3.2: Axial locations of pressure transducers

3.2.2 Inlet

The conical forebody is the second major component that makes up the inlet assembly. The inlet forebody has a half angle of 12.28 degrees and has a total length of 347.57 mm. The forebody has five holes drilled and tapped along the centerline of the inlet surface. These holes are potential locations for pressure transducers and they are all used for this work. The locations of these holes can be seen in Figure 3.2.

Issues associated with the pre-existing condition of the inlet forebody are:

- There are large gaps on the inlet surface around the pressure transducer holes
- Previous methods of mounting the cowl to the inlet have left two cut out slots running along a section on the top side of the inlet

To fix the large gaps around the transducer mountings two possible solutions were considered; epoxy filler and press fitting some aluminum slugs and redrilling the holes. It was decided that the optimum solution was to use epoxy filler to fill in the gaps. The reason this was chosen is because epoxy filler is much easier to apply and much easier to sand back to the original conical shape. Also, if aluminum slugs were used the inlet would need to go back to a machine shop to have the holes re-drilled and tapped. Like the cowl, the two cut out slots on the inlet will be filled with epoxy filler and sanded back to the original shape so that the flow will not be disturbed.

3.2.3 Setup

The current set up consist of a base mount structure that gets bolted to the base of the test section. This mount then holds a 25mm shaft which in turn supports the inlet. This entire mounting structure will be able to be utilised when the testing associated with this project takes place.

3.3 Initial Concepts

This design will have two main features that can be designed and decided upon separately. These are:

- Guidance and mounting system
- Actuation system

3.3.1 Guidance and Mounting System

There were four main concepts investigated for a guidance and mounting system. These were:

1. A number of hollow tubes placed so that the contact between the hollow tubes and mounting shaft caused the cowl to stay aligned.
2. The pre-existing method of attaching the cowl incorporating longer slots and a leading edge on the mounting plate
3. A machined collar that will slide over the mounting shaft and attach to the cowl by two mounting brackets
4. A modified version of the initial method of mounting the cowl as designed by Harland (2012).

Concept 1

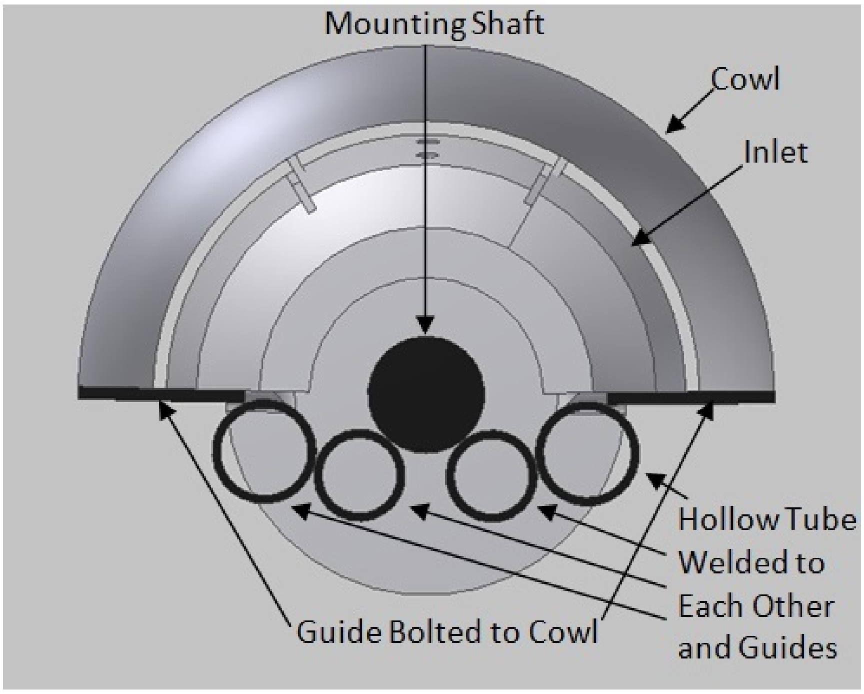

Figure 3.3: Sketch of Concept 1

This design consists of two guide brackets that are bolted to the cowl and have a leading edge machined into them. These bolted brackets utilise the existing holes in the bottom face of the cowl and the leading edge is incorporated to reduce the disturbance of the flow. On the inside edge of each bracket there is a length of tube that is welded in place. This tube is then welded to another length of tube so that the inner most tubes rub up against the mounting shaft. The contact between the inner tubes and the mounting shaft is the mechanism that guides and mounts the cowl axially, while the guide brackets will guide the cowl in the radial direction. A concept sketch of this design can be seen in Figure 3.3.

The advantages of this design are:

- There are not too many components
- The cowl and inlet do not need to be modified in any way

The disadvantages of the design are:

- Extremely hard to manufacture due to trying to orientate the tube sections properly and the fact that the flat surface on the cowl and inlet are actually at an angle of 178 degrees, not 180 degrees.

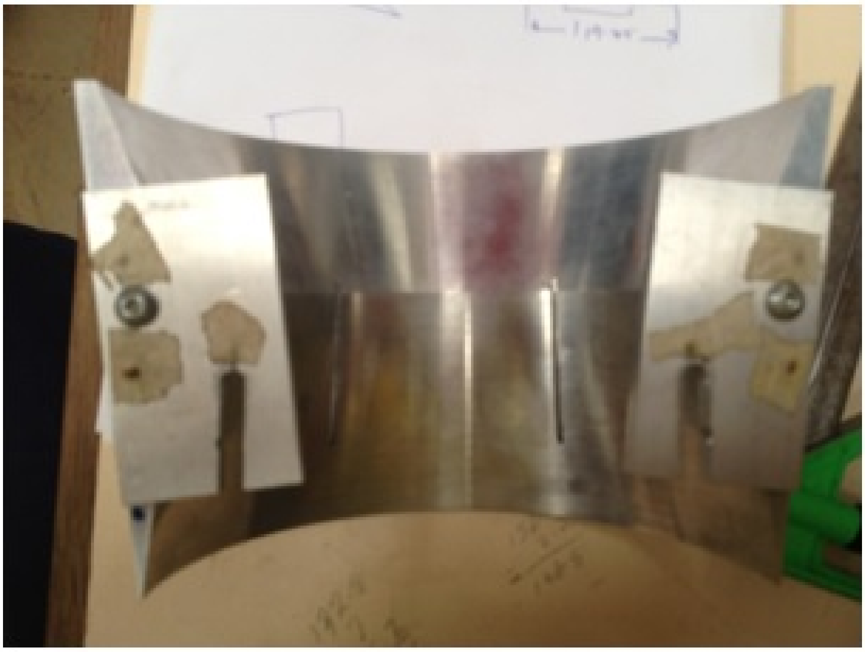

Figure 3.4: Picture of Concept 2

- Deflection caused by self weight is likely which will cause the cowl mounting to be unsteady and loose.
- Because thin materials are needed to reduce weight and size, deflection from the welding process is also likely which will cause the cowl mounting to be unsteady and loose.

Concept 2

The second guidance and mounting design concept is a simple modification of the pre-existing mounting system. As you can see from Figure 3.4 the current mounting system consists of two guide brackets that are bolted to the cowl. These brackets then have a slot cut into them which lines up with a bolt that is in the inlet. The current problems with this method of mounting the cowl are; the guide brackets have a flat leading face on them that disturbs the flow and the slots in the bracket are not long enough to provide room for adequate actuation. The modifications that would be made to allow this system to be used in this project are; a sharp leading edge would be put on the leading face to reduce the disturbance to the flow and the slots would be made longer.

The advantages of this design are:

- It utilises an existing guidance and mounting system

- There is only two components

The disadvantages of this design are:

- It would be hard to a smooth actuation because equal force would need to be applied to each mounting bracket at the same time.

Concept 3

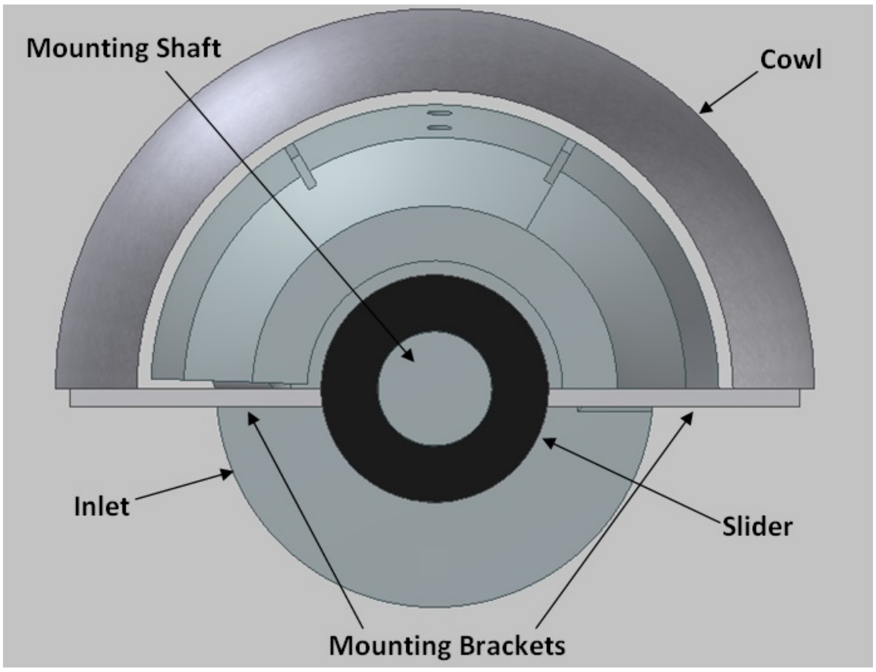

Figure 3.5: Sketch of Concept 3

Like concept 1, this concept would utilise the main mounting shaft as its main method of guidance. This design would consist of a machined part that would slide over the mounting shaft that is connected to the cowl via two mounting brackets. These mounting brackets bolt into the existing holes in the cowl and bolt to the central collar. These brackets would also have a sharp leading edge to prevent excess disturbance to the flow. As mentioned earlier, the mounting shaft would guide the cowl axially and the mounting brackets would guide the cowl in the radial direction. A concept drawing of this method can be seen in Figure 3.5. The advantages of this design are:

- This design would be very stable because it is possible to get a good fit on the shaft
- The mechanical design of this method is relatively simple

- Easy to assemble

The disadvantages of this design are:

- Machining is required

Concept 4

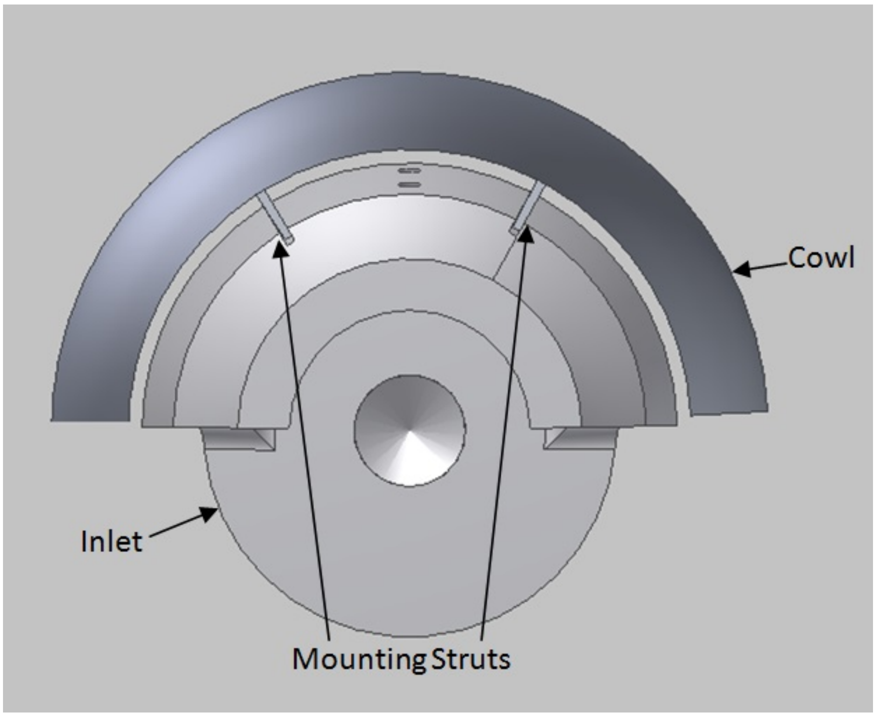

Figure 3.6: Sketch of Concept 4

Design concept 4 involves the recreation and modification of the original method of mounting the cowl designed by the original designer of the inlet. In this system the cowl and inlet both have grooves cut into them where struts are placed, as seen in Figure 3.6. The modification that is required is that the slots need to be longer and deeper. The slots need to be longer to allow for the actuation of the cowl. Also, the slots need to be deeper because in the previous design there was a hole through the inlet in the grooves that allowed the struts to be mounted securely. Since the design required for this work needs the cowl to be able to move this is not an option so the grooves need to be deeper overall to support the cowl properly. The advantages of this design are:

- Utilise the existing slots

The disadvantages of this design are:

- There will be gaps in the inlet where the slots aren't being filled
- The struts are in the flow
- It is possible that the mounting won't be very stable
- It will be very hard to integrate and actuation system with this design

3.3.2 Actuation System

When considering the design for the actuation system three main concepts were investigated: These concepts were:

1. Pneumatic system
2. Electronic system
3. Spring system

Concept 1

The idea of a pneumatic system requires that there be area for the pressurised air to act upon and requires adequate sealing of the system. The reason the system needs to be properly sealed is because if it isn't air will be able to escape during the test and interfere with the test section flow. The way that a pneumatic system can be integrated with each of the guidance systems is:

- Guidance and mounting concept 1. A cap of would need to be welded into at least two of the hollow tubes, to allow for an equal force either side of central shaft. A special fitting would need to be made so that can be inserted into the hollow tubes and allow air to be delivered into a cavity pushing the cowl forward.
- Guidance and mounting concept 2. It would be difficult to use a pneumatic method of actuation for this design. The reason for this is because there is not much area available that a pressure could be applied to. The only way a pneumatic system could be implemented into this design is if another connecting part was made so that there was a face that pressure could be applied to.

- Guidance and mounting concept 3. This design would be by far the easiest to implement a pneumatic actuation system. Concept 3 has a face where pressure can act that is located on the center plane of the cowl. To utilise this face a fitting would need to be made that slides over the mounting shaft and also slides over the collar. This would allow for a cavity that could be pressurised to propel the cowl forward.

- Guidance and mounting concept 4. This would be very difficult to apply a pneumatic system of actuation to. The reason being that there is no faces to apply pressure and there are no components of the design that are not in flow of the test section.

The advantages of a pneumatic system are:

- Can be relatively simple
- The actuation speed can be controlled by regulating the pressure
- Reliable

The disadvantages of a pneumatic system are:

- Depending on the force required to actuate the cowl at the required speed a large area may be needed to achieve this.

Concept 2

For an electronic system to work there would need to be enough room to fit a linear actuator in the form of a power screw. The most efficient way of fitting the actuator would be to make a clamp to fix it to the mounting shaft. The ways this system could be integrated with each of the guidance and mounting system concepts are:

- Guidance and mounting concept 1. To fit an electronic method of actuating the cowl to this design the best method would be to connect a linear actuator to the two inside sections of hollow tube. This would allow for an equal force either side of the central shaft allowing a smooth actuation.

- **Guidance and mounting concept 2.** The best way to fit a linear actuator to this design would be to connect the two mounting brackets via another bracket and have the actuator act in the center of it. Because the shaft would interfere with a straight bracket, the bracket would need to either have a hole in it that goes over the shaft or just bend around it.

- Guidance and mounting concept 3. To integrate an electronic system into this design a bar or piece of flat would need to be mounted off the central sliding part to allow a place for the actuator to act.

- Guidance and mounting concept 4. This would be very difficult to mount a linear actuator to. The only way it would be possible is if the slots in the inlet went all the way through so something can be attached underneath them. If the slots came all the way through a piece of flat or bar could then attach to the bottom of the struts and connect inside the inlet allowing a place for the actuator to act.

The advantages of an electronic actuation system are:

- There would only need to be a few components involved
- There would be the ability to control the speed of actuation

The disadvantages of an electronic actuation system are:

- Hard to reach speeds as high as the pneumatic system
- The devices would wear out quickly when operating at such high speeds and exposed to sudden stoppages.
- Because of the high forces and speeds involved all the shafts and brackets would need to be quite large to prevent buckling failure

Concept 3

Concept 3 is basically the same as concept 2 except that instead of a power screw a spring loaded cylinder would be used. This spring system would require another method of setting it off, such as an electrical or pneumatic signal. The advantages of a spring loaded cylinder are:

- The system has the potential to be quicker than the power screw
- A spring system would be more durable than an electrical system in this particular testing environment

The disadvantages of using a spring loaded cylinder are:

- Could be unreliable
- This application would require a stiff spring and this may cause trouble trying to reload it

3.4 Design Choice

To make sure the chosen design is the most effective and best suited for this application a decision matrix will be used. The more important of the two required features for this design is the guidance and mounting system. The reason for this is because the performance of the actuating cowl as a whole system will depend on how easily and effectively the cowl moves not how it is actually moved. Therefore the guidance and mounting system will be decided upon first and then the actuation method will be chosen depending on the outcome of the first decision.

3.4.1 Guidance and Mounting System

The qualities the guidance and mounting design must possess are:

- Must not affect the test section flow
- Must be stable
- Potential actuation distance
- How easily the design can be manufactured and assembled

The allow a decision to be made more effectively each required attribute is given a rating of importance with the sum of all rating to equal 1.

Table 3.1: Guidance and mounting system concept weighting

Attribute	Weighting	Reason
How much it affects test section flow	0.4	If the flow is affected results are invalid
Actuation stability	0.3	The cowl needs to actuate smoothly for best results
Actuation distance	0.1	Less important because all designs will be able to move the minimum distance
Ease of manufacture and assembly	0.2	If it cannot be made or assembled it cannot be used

This decision matrix will be calculated by giving each concept a score 1-10 where the score 10 will be the best performing concept in that area. This score will then be multiplied by the weightings chosen in Table 3.1. Therefore the best design will be the design with the highest total score.

Table 3.2: Guidance and mounting system concept decision matrix

	Weighting	Concept 1	Concept 2	Concept 3	Concept 4
Test section flow	0.4	9	9	10	2
Actuation stability	0.3	6	8	10	4
Actuation Distance	0.1	10	10	10	3
Ease of manufacture / assembly	0.2	2	10	9	4
Total	1	6.8	9	9.8	3.1

As you can see from Table 3.2 the best design choice for the guidance and mounting system is concept 3, which is a machined collar that will slide over the mounting shaft and attach to the cowl by two mounting brackets.

3.4.2 Actuation System

The qualities that are important and that the actuation systems will be critiqued against are:

- Ability to be fitted to chosen guidance and mounting design
- Actuation speed
- Actuation reliability
- Durability of design

Like section 3.4.1 each quality will be given a rating and score to determine which system is best suited to this application. Table 3.3 shows the chosen weightings

Table 3.3: Actuation system concept weighting

Attribute	Weighting	Reason
Compatibility with chosen guidance and mounting system	0.3	It needs to be fitted to the chosen guidance and actuation system
Actuation speed	0.3	The test only runs for 200ms so the actuation needs to happen quickly
Actuation reliability	0.2	It takes a while to get the tunnel ready for a run so it needs to run how its suppose to every time
Durability of design	0.2	The design needs to last for at least as long as all testing for this project takes place

Table 3.4: Actuation System Concept Decision Matrix

	Weighting	Concept 1	Concept 2	Concept 3
Compatibility with chosen guidance and mounting system	0.3	10	9	9
Actuation Speed	0.3	10	7	8
Actuation Reliability	0.2	10	5	7
Durability of Design	0.2	10	5	7
Total	1	10	7.4	7.7

Therefore, from Table 3.4 it can be seen that the actuation system most suited to this application is a pneumatic system.

Table 3.5: Limitations of design

Component	Limitation
Collar	Front face needs to be large enough so that a large enough force can be applied to reach the required acceleration
Collar / pressure fitting	The collar needs to fit inside the end of the pressure fitting
Pressure fitting	The diameter of the entry to underneath the inlet is 56mm. Therefore the outside diameter of the pressure fitting must not exceed this
Collar / Pressure fitting	The cavity created between the two needs to be completely sealed so no air can escape

3.5 Component Design

As discussed in section 3.4 the guidance and actuation system will consist of a central collar that slides over the mounting shaft. This part will then be mounted to the cowl by two brackets and all this will be driven by a pneumatic actuation method. The components that will be required for this design are:

- Collar
- Two mounting brackets or ‘wings connecting the slider to the cowl
- A mechanism of locking the cowl into position when static tests are carried out
- A mechanism that will bring the cowl to a stop when under dynamic conditions
- An air fitting that locks onto the shaft and connects with the collar to create a sealed cavity. This piece must be able to connect to a pressurised air supply
- A bracket that the pressure transducers can be mounted on

The limitations and boundaries of this design, as listed in table 3.5, will be addresses first and the other components worked out around them.

3.5.1 Actuation Force Requirements

The test only lasts for 200ms, therefore is it essential that the actuation be as quick as possible. The larger the front face of the collar, the larger the applied force can be which means the higher the acceleration. Initial sizing estimates are calculated assuming:

- An actuation time of 15 milliseconds
- An actuation distance of 35mm
- Delivery pressure of 1MPa (pressure can be regulated but 1 MPa is easily achieved)
- Estimated weight of 2 kg. (Cowl mass weighed and equals 700g alone).

The acceleration needed to travel the required distance in the required time is found by using a general motion equation (Hibbeler 2010) assuming constant acceleration. Using equation 3.1 and assuming the collar initially starts off at rest the acceleration is worked out to be 311.11 m/s.

$$S = S_0 + v_0 t + \frac{1}{2} a t^2 \tag{3.1}$$

The force required to push the collar along was calculated so that the required surface area needed for the pressure to act could be worked out. The required force was worked out using a static coefficient of friction, for mild steel on mild steel, of 0.62. Using equation 3.2 the force required was determined to be 634.4 N.

$$F - F_f = ma \tag{3.2}$$

Since we are working off the fact that the pressure will be 1 MPa, using P = F/A, the required area for the pressure to act is calculated to be 634.4 mm^2. Knowing that the shaft this part fits over is 25 mm in diameter, the required diameter is calculated to be 57.5 mm using equation 3.3.

$$A = \pi r_o^2 - \pi r_i^2 \tag{3.3}$$

As you can see from equation 3.3 the resulting diameter is 1.5 mm greater than the limit. It will be fine to make this diameter a little bit less because it is unlikely it will need to travel the full 35 mm and it doesn't need to do it in exactly 15 milliseconds.

Table 3.6: O–Ring specifications (StandardsAustralia 1986)

O-ring Size Number	Section Diameter (mm)	To Fit
210	3.53	24.4mm bore
225	3.53	47.63mm shaft

3.5.2 Sealing of Design

The airflow in the test tunnel must not be disturbed during the test for optimum results which means that the cavity filled with the pressurised air must be perfectly sealed or must divert the leaked flow out the back of the inlet. Many different methods of sealing the design were considered, these included:

- O-rings
- Gaskets and backing plates
- Wiper seals of different profiles

O-rings were chosen as the final choice for sealing the design. The reasons for choosing o-rings were:

- O-ring design is simple
- O-rings are more than capable of handling dynamic sealing conditions
- O-rings are readily available and easy to assemble

Referring to AS2842 -1992, an o-ring with size number 210 was chosen for between the shaft and components and an o-ring with size number 225 was chosen for between the two components. The specifications of the selected o-rings can be seen in Table 3.6.

After the o-rings were chosen AS2842-1992 was used to calculate the required geometric sizes of the two center shaft bores and the two ends of the components that fit together. The final sizes were calculated assuming that all fits will be exposed to dynamic conditions even though only two out of three are. This was done for two reasons; first reason to allow the two groove sizes in the 25mm bores to be equal and secondly to make it easier to assemble. The reason this needs to be easy to assemble is because the inlet

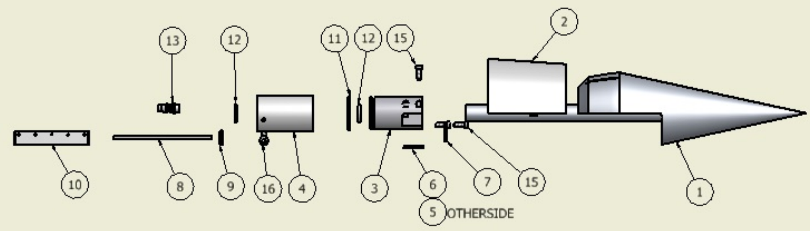

PARTS LIST		
ITEM	QTY	PART NUMBER
1	1	Inlet
2	1	Cowl
3	1	Collar
4	1	Pressure Fitting
5	1	Left Side Mount Plate
6	1	Right Side Mount Plate
7	1	Guide Plate
8	1	Guide Rod
9	1	Stop
10	1	Transducer Bracket
11	1	O-ring 225
12	2	O-ring 210
13	1	Pneumatic Fitting (Representation Only)
14	2	M5 x 1.8 x 16 Countersunk
15	6	M6x1 x 16 Socket Head Cap Screw
16	1	M8x1.25 x 25 Socket Head Cap Screw

Figure 3.7: Exploded drawing of final design

assembly will need to be disassembled and reassembled many times and because there are many sharp edges involved the harder it is to force the component onto the shaft the easier it will be to slip and cut yourself.

3.6 Final Design

Figure 3.7 shows the final design of the actuating cowl assembly. The manufacturing drawings of each part can be seen in Appendix B. As you can see there are ten main components involved:

1. Inlet forebody
2. Cowl
3. Collar
4. Pressure fitting
5. Left mount bracket
6. Right mount bracket
7. Guide plate

8. Guide rod

9. Stop

10. Transducer bracket

The main features of the overall design that are influential to inlet performance are easiest described by categorising them into the respective components.

Collar main features. The main features of interest in the collar are the length and the diameter. The collar was designed so that it could potentially allow 42 mm of room for actuation. This is an overestimate of the actuation that is going to be required because it might be difficult to position the pressure fitting exactly where its needed due to clashing of components. The final diameter was reduced from 57.5 mm to 49.86 mm so that there is more clearance between the collar and the inlet body. This is acceptable because as outlined in section 3.5.1, it is allowable for the cowl to take a little longer than calculated to accelerate and also the pressure input is adjustable.

Pressure fitting main features. The design of the pressure fitting is fairly straight forward where it acts like the bore and the collar a piston. This component, like the collar, was designed so that there is extra room for movement (55 mm in total). The pressure fitting is held stationary on the shaft with the use a M8 bolt and air is delivered into the cavity through a standard 1/2" BSP pneumatic fitting.

Mount brackets main features. The only important features of the mounting brackets that add to the overall inlet performance are the leading edge and the countersunk fasteners. This features allow these components to cause as little interference to the flow as possible which will decrease the chance of inconsistent results.

Stop main features. The main feature to be recognised about the stop is the layer of rubber on the impact surface. This layer acts as a dampening mechanism when the guide plate hits the stop. The reasoning for the damping is because in preliminary testing is was found that the impact between the original stopper and the guide plate caused permanent deformation of the guide plate, which on inspection looked like it would most likely eventually fail. The rubber layer is not ideal because it tends to cause the cowl to vibrate at the end of travel. If more time was available this would be investigated further.

The chosen method of operating the inlet inside the test section was by using a standard 12V solenoid valve. To operate the test tunnel the test section must be evacuated to a pressure of somewhere below 850 Pa. During preliminary testing it was found that when the tunnel was evacuated the seal between the collar and pressure fitting was great enough that an atmosphere pressure would be trapped in the cavity. The pressure differential between the cavity and the test section caused the collar to slide forward prematurely. To counter this a tee fitting was added between the solenoid valve and the pressure fitting with a needle valve coming off the center branch. This needle value allowed the cavity to bleed and equalize with the test section. This solution meant that when the pressure was engaged to push the collar air would be able to escape the cavity. To limit the effects this might have on the experiment the needle valve was directed downstream so that no disturbance to the flow occurred.

Chapter 4

Experiment Design

This chapter outlines the testing parameters and describes the equipment used while testing this inlet. All experiments were undertaken in the TUSQ facility located at the University of Southern Queensland, Toowoomba.

4.1 Testing Environment and Equipment

The hypersonic wind tunnel facility used in this work, known as TUSQ, is a light free piston compression tunnel. The barrel of the facility is 16m long and has an internal diameter of 130mm. For this work a Mach 6 contoured nozzle with an exit diameter of 217.5mm was used. A schematic of the facility can be seen in Figure 4.1. To operate the tunnel the test section is evacuated to a pressure somewhere below 1000Pa absolute (usually 650-900Pa). Once the test section has been evacuated high pressure air (3MPa gauge for this work) was used to drive a nylon piston down the barrel compressing the test gas in an almost isentropic manner (Buttsworth 2009). This compressed air then ruptures a 100 μm thick diaphragm and flows through the nozzle.

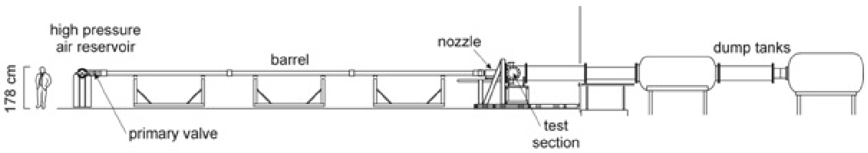

Figure 4.1: Schematic of TUSQ hypersonic facility (Buttsworth 2009)

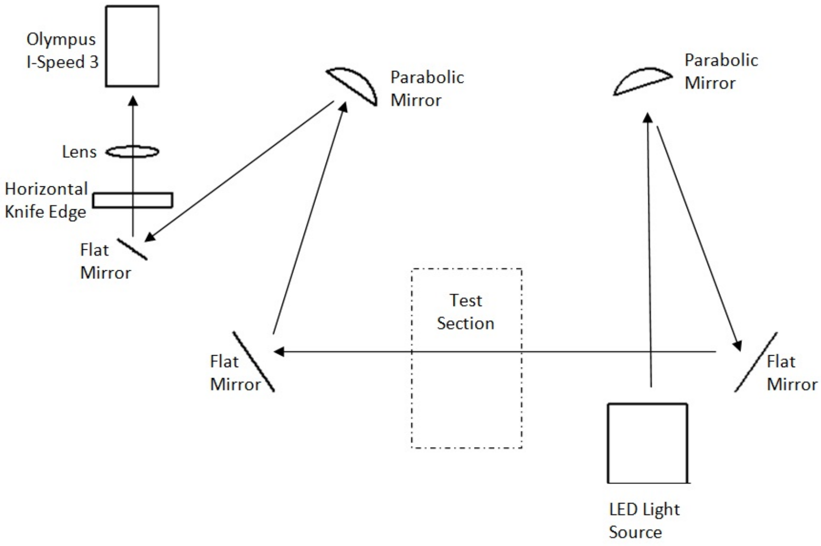

Figure 4.2: Schlieren flow visulisation setup

4.2 Required Data

The data that was collected for the testing of this inlet was pressure measurements from the surface of the inlet, pressure measurements from inside the barrel (approximately 130 mm upstream of the nozzle) and Schlieren flow visulisation. The pressure readings from the surface of the inlet and the flow visualisation allow the performance of the inlet to be evaluated while the pressure readings inside the barrel allow the performance and flow characteristics of the tunnel run to be evaluated.

The Schlieren flow visulisation setup that was used for these experiments can be seen in Figure 4.2. As you can see the light source gets reflected and focused through the test section by a series of parabolic and flat mirrors before going through a horizontal knife edge, a lens and finally into the camera. The light source used is a red LED which was run at 15.5 V. The horizontal knife edge was positioned so that it cut out just below half the light, allowing density gradients to be seen more clearly. The imagery was captured at 2000 frames per second (fps) by an Olympus I-Speed 3.

The surface pressure readings are taken in five different locations on the inlet. These locations are defined in section 3.2.2 and can be seen in Figure 3.2. Three different types of pressure transducers were used; SensorTechnics BSDX1000A2R locations 1, 2 and 3, SensorTechnics BSDX2000A2R location 4 and SensorTechnics BSDX5000A2R location 5. Three different types of pressure transducers were used because these were

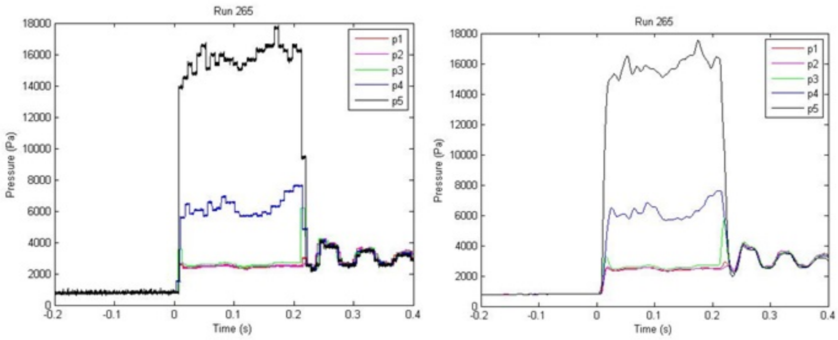

Figure 4.3: Unfiltered data (left) compared to filtered data (right) (run 265 shown)

the only available transducers that suited this application. These transducers were connected to transducer fittings in the tapped locations by small pneumatic tubes. The pressure transducers are then bolted to a bracket running underneath the inlet. The data acquisition system was setup to take measurements at 10,000 readings per second. A total of 30,000 points of data were taken each transducer each run with 15,000 readings taken pre-trigger. Atmospheric readings were taken before the very first run and after the very last run to ensure that sensitivities (V/Pa) of each transducer remained constant throughout the testing.

Figure 4.4 shows a typical plot of the barrel stagnation pressure history. As you can see the test run is only a small proportion of the plot, approximately 200 ms. The results from this pressure transducer allow the Mach number, temperature and velocity of the flow to be calculated.

Once the data was collected it was obvious that there was a lot of internal noise coming from the transducers. To address this problem a butterworth filter (MathWorks 2013) with a cutoff frequency of 50Hz was run over the results to 'smooth' them out. Figure 4.3 compares the before and after of a data set with the butterworth filter applied. From Figure 4.3 it is obvious that the butterworth filter improves the quality of the data and makes it a lot easier to read.

4.3 Kantrowitz Limit

The Kantrowitz limit was used as a starting point for these test runs. Mentioned earlier in section 2.3.2 the Kantrowitz limit is an estimate of the contraction ratio that will

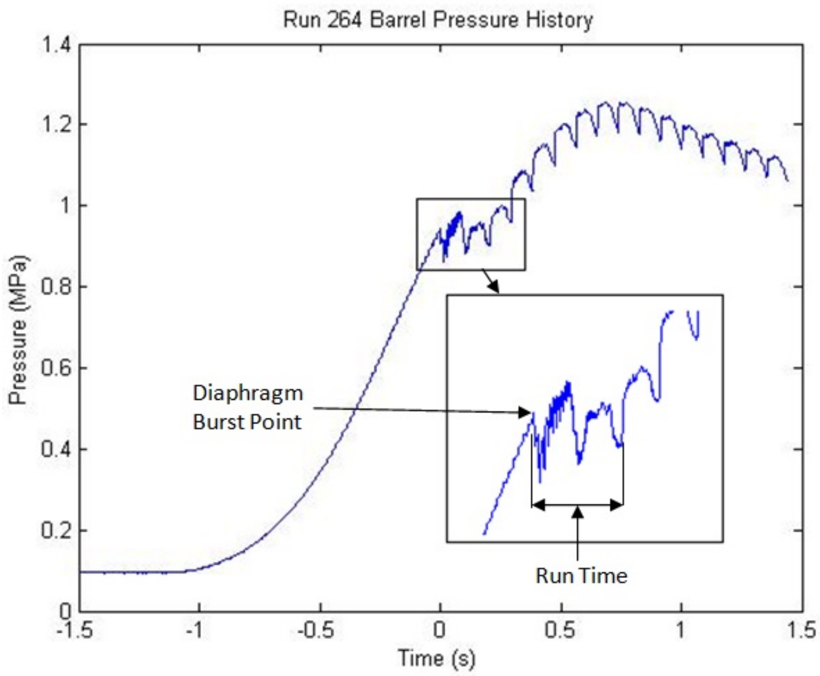

Figure 4.4: Barrel pressure history (run 264 shown)

allow the engine to self start. The Kantrowitz limit is defined in equation 2.1.

The Kantrowitz limit for this inlet was calculated assuming a Mach number of 5.85 and a ratio of specific heats, γ, of 1.4. substituting these values into equation 2.1 the calculated Kantrowitz limit for these operating conditions is 1.5723. In essence, the inlet entry area must be 1.5723 times the inlet throat area to suit the Kantrowitz limit for these operating conditions.

Matlab was used to calculate where the cowl would need to be positioned so that the inlet was setup at the Kantrowitz limit. The method in which the Matlab script calculates where the Kantrowitz limit is represented in the flow chart shown in Figure 4.5. The inlet compression geometry was the only geometry modeled and simulated in this code because it is the only geometry that affects the Kantrowitz limit. The inlet compression geometry can be seen in Figure 4.6 and model outputted by Matlab can be seen in Figure 4.7.

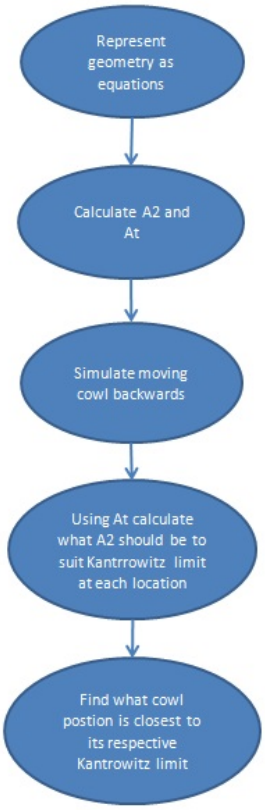

Figure 4.5: Flow chart representing Kantrowitz limit calculation

4.4 Cowl Testing Positions

There were two methods utilised when the cowl testing positions were chosen; test at the Kantrowitz limit and start testing at a previously tested position and depending on the results choose the next position accordingly. The desired outcome for the static cowl tests is to determine where the inlet starts and unstarts. Once this is determined a dynamic test can be undertaken where the cowl is actuated from a point where the inlet starts through to a point where the inlet unstarts.

This particular inlet was tested at different angles of attack by David R. Buttsworth in August 2011. The location of the cowl during these tests will be the starting point for this lot of testing. For simplicity this position was defined as the zero position. The zero position is defined in Figure 4.8. The location of the cowl in each test run can be seen in Table 4.1.

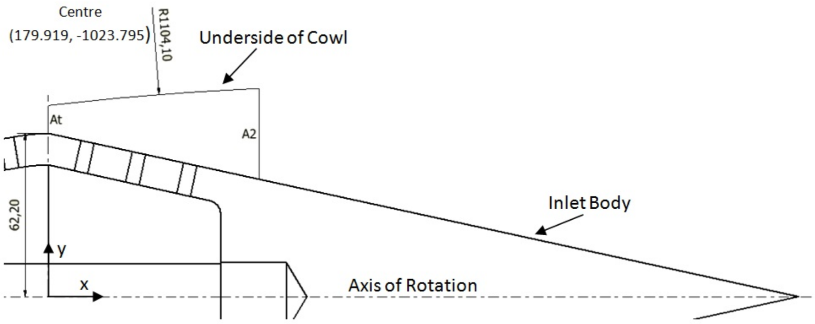

Figure 4.6: Sketch of the Inlet Compression Geometry

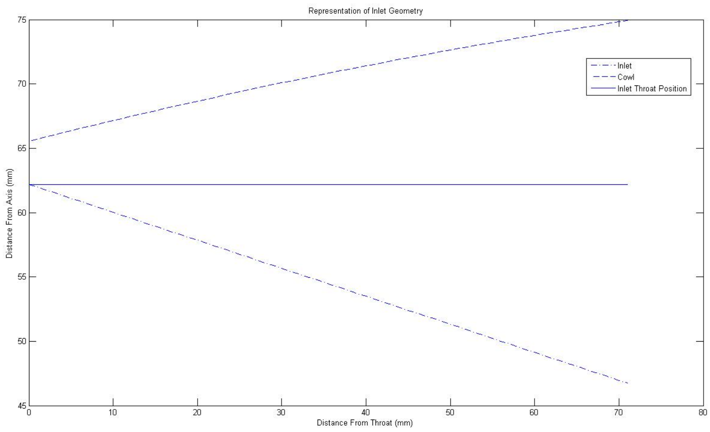

Figure 4.7: Inlet and Cowl Matlab Model

Table 4.1: Location of the cowl for each run

Run Number	Location (mm) reference to figure 4.8
264	12.3 (Calculated Kantrowitz limit)
265	12.3 (Calculated Kantrowitz limit)
266	0
267	9.7
268	10.1
269	13
270	15 to 0 (Dynamic test)
271	15 to 0 (Dynamic test)

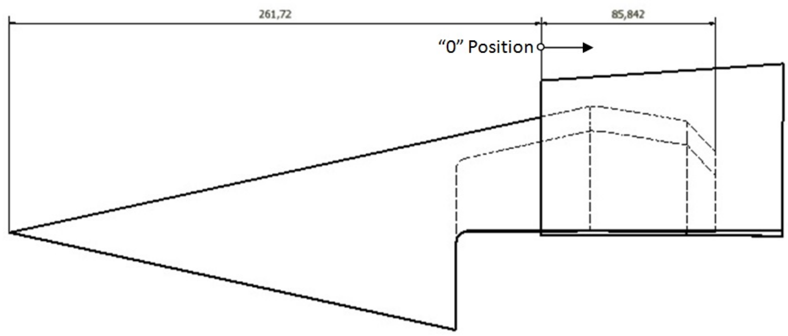

Figure 4.8: Physical location of zero position

Chapter 5

Results and Discussion

5.1 Introduction

To evaluate the performance of this inlet under both static and dynamic cowl conditions a total of eight test runs were carried out. The operating conditions of each test run can be seen in Table 5.1. For each run the piston (approximately 350 grams) was driven by a pressure of 3MPa.

Seven out of the eight runs were successful (run 270 was unsuccessful) and both Schlieren flow visulisation and pressure measurements were taken for all runs except for run 264 which only had pressure measurements and run 269 which only has Schlieren images collected. This chapter will analyse and evaluate the results from the test runs.

5.2 Flow Conditions

The Mach number, temperature and velocity of the flow for each run was calculated to define the flow conditions. A summary of the flow conditions can be seen in Table 5.2. All calculations are done assuming isentropic relationships and assuming the air behaves like as ideal gas. The stagnation pressure, P_o is taken as an average of the barrel stagnation pressure over the first 50 ms of flow. The Mach number was calculated using equation 5.1 (Pritchard 2011) assuming P is equal to P_i (Table 5.1) and γ is constant and equal to 1.4.

Table 5.1: Operating conditions of each run

Run Number	$P_{atm}(kPa)$	T_{amb} ($°C$)	$P_i(Pa)$
264	94.72	24.8	810
265	94.13	27	790
266	93.58	17	640
267	93.58	20	670
268	93.24	27	720
269	93.52	25	800
270	93.52	27.5	710
271	93.52	27.5	710

$$\frac{P_o}{P} = \left[1 + \frac{\gamma - 1}{2} M^2\right]^{\frac{\gamma}{\gamma-1}} \tag{5.1}$$

From previous work the temperature at the nozzle inlet is known to be approximately 560 K. Temperature of the flow was calculated using equation 5.2 (Pritchard 2011) assuming; T_o equal to 560 K, M equal to Mach number calculated in equation 5.1 and γ equal to 1.4.

$$\frac{T_o}{T} = 1 + \frac{\gamma - 1}{2} M^2 \tag{5.2}$$

Once the temperature of the flow is known, equation 5.3 (Pritchard 2011) can be used to calculate the speed of sound in these particular conditions.

$$c = \sqrt{\gamma R T} \tag{5.3}$$

Using the values from equation 5.1 and equation 5.3 the velocity of the flow can be worked out using equation 5.4 (Pritchard 2011).

$$M = \frac{v}{c} \tag{5.4}$$

5.3 Inconsistencies in Results

During the testing it came apparent that there was one main issue with the inlet that could possibly affect the results and outcomes of the test runs. The issue, which was

Table 5.2: Flow Conditions

Run Number	P_o (kPa)	M	T (K)	v (m/s)
264	920.8	5.69	75.0	987
265	926.8	5.72	74.3	988
266	927.6	5.92	70.0	992
267	931.7	5.88	70.8	991
268	920.0	5.80	72.6	990
269	0	0	0	0
270	919.5	5.81	72.3	990
271	946.3	5.84	71.7	990

visually picked up in the Schlieren flow visualisation, is the fact that the cowl tends to 'rock' backwards and forwards during the run. This rocking action causes the leading edge of the cowl to move up and down in the flow. This movement obviously affects the contraction ratio which means it isn't plausible to draw definite conclusions on static locations. In essence, saying that the inlet starts or unstarts at an exact location cannot be validated but it can be used as an estimate. However, the dynamic cowl conditions can be validated because all runs will experience the same movement and the dynamic condition's main objective is to investigate whether or not the actuation of the cowl can differ the results at the same locations of the static tests.

This rocking motion was investigated via the analysis of the Schlieren footage and it was found that the amount of movement was approximately 1.7 mm. After measuring the hole in the collar and the shaft, it was found that the hole was actually 25.35 mm diameter even though it was specified at $25.14^{+0.15}_{-0.10}$, and the shaft was exactly 25 mm. This is a small manufacturing error that would cause some of the movement but it is now obvious that the specified tolerance could have possibly had almost the same affect with the upper limit being 25.29 mm.

The worst case scenario when the collar is tipped all up the clearance at the end of the collar would be 0.35 mm. Using the geometry of the assembly, 0.35 mm at the end of the collar tipped back equates to 0.55 mm at the leading edge of the cowl. The rest of the movement in the cowl can be accounted for by deflection in the mount brackets.

The deflection in the brackets can be calculated using the angle of twist equation shown in equation 5.5. This calculation assumes that the brackets are rectangular bars (ignoring the leading edge) and the torque is shared evenly between them. The force acting on the cowl to cause the deflection is the drag force of the cowl.

$$\phi = \frac{TL}{c_2 a b^3 G} \tag{5.5}$$

To simplify the calculation, the pressure acting on the cowl is assumed to be constant and equal to the largest pressure measured in a run. Referring to run 265, the largest pressure measured was approximately 18 kPa. Therefore, using equation 5.6 and knowing the largest cross section of the cowl is equal to 6576 mm^2 the drag can be worked out to be 118.37 N.

$$DragForce = PA \tag{5.6}$$

Assuming the force acts at the center of gravity of the cowl (46.7 mm above the axis) the torque on the brackets can be worked out to be 5.53 N.m using T = Fd. Using equation 5.5 and assuming G is equal to 77.2 GPa (Beer 2009), a is equal to 0.015 m, b is equal to 0.004 and c_2 is equal to 0.281 (Beer 2009), the angle of twist is 0.479°. Where a and b are the width and thickness of the bracket.

Knowing the leading edge of the cowl is 69.14 mm away from the axis of twist, the movement at the leading edge can be worked out geometrically to be 0.58 mm. Therefore the combined movement from the clearance and the deflection is approximately equal to 1.13 mm. It is reasonable to assume that the remainder of the movement is caused by movements in the joins and the inaccuracies in the theoretical calculations.

In summary, the most likely causes for the rocking action of the cowl are:

- Too much clearance between the collar and shaft (design was flawed from the start)
- Deflection in the mounting brackets from the drag force
- Movement in the joins of the assembly

Table 5.3: Summary of static cowl runs

Run Number	Result
264	Started
265	Started
266	Did not start
267	Did not start
268	Did not start
269	Started

5.4 Static Tests

The static tests that were carried out were runs 264 through to run 269. As mentioned previously the main objective for the static tests was to simply understand where the inlet self starts and where it doesn't. A summary of the results for the static cowl conditions can be seen in Table 5.3.

As shown in table 5.3 runs 264, 265 and 269 all appeared to start while the remainder did not. Figure 5.1 shows the comparison of a started run (265) versus an unstarted run (267). Run 265 is flowing relatively smoothly apart from slight separation of the boundary layer close the to cowl while run 267 the boundary layer has fully separated and the flow can be seen spilling out and around the cowl. The slight separation of the boundary layer close to the cowl can be seen in every started run and the most likely cause for this is a transducer fitting could be tripping the boundary layer. Further investigation would be required to confirm this. It is also noticeable during the flow visulisation that oblique shock from the cone in run 265 is unsteady at times. The pressure measurements of run 264, which was tested at the same location, also indicate some unsteadiness with the pressures 1, 2 and 3 starting to differ from one another towards the end. This is an indication that this cowl position is close to unstarting. This is expected at this location because it is the Kantrowitz limit. Run 269 was done 0.7 mm further back and the unsteadiness of the shock seemed to disappear.

Figure 5.2 shows the comparison of pressure measurements of runs 267 and 265. The plots shown indicate what has already been seen from the flow visulisation, run 265 started while run 267 did not. If the flow around a cone is steady in hypersonic flow the

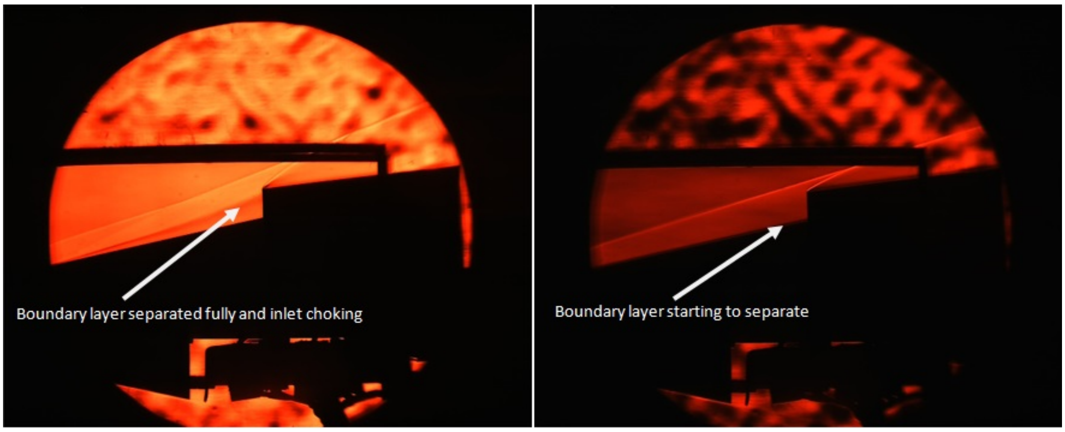

Figure 5.1: Flow visulisation of runs 267 (left) and 265 (right) taken 100 ms after the start of the flow

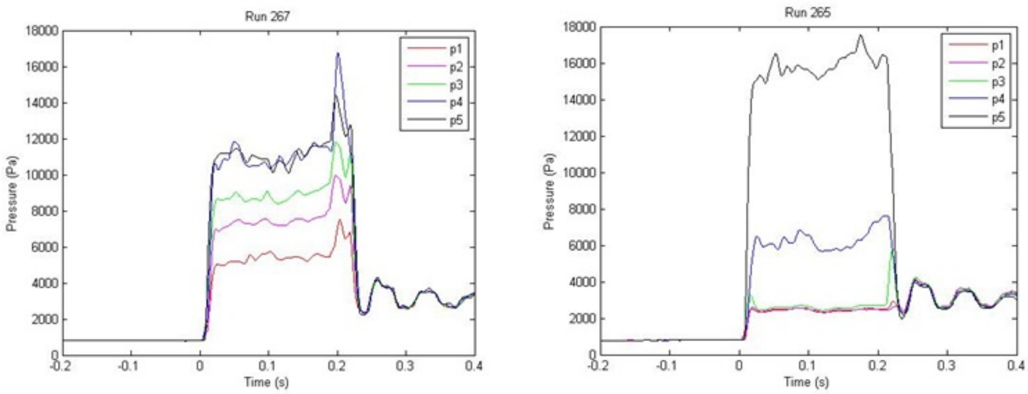

Figure 5.2: Pressure measurements of runs 267 (left) and 265 (right)

surface pressure should be uniform along the cone. Recall that pressure transducers 1, 2 and 3 are the only transducers located along the cone while the other two are located inside the inlet. Therefore for the flow to be steady and the inlet started transducers 1, 2 and 3 must be the same, which is shown in Figure 5.2.

5.5 Dynamic Test

A single dynamic test was carried out to investigate the effects it would have on the starting abilities of this particular inlet. Run 270 will be excluded from the results because the cowl actuated prematurely and no results were acquired for a dynamic cowl condition. To analyse the dynamic condition using the flow visulisation the image of static tests (runs 266, 268 and 269) were compared to the image of the dynamic test at the instant the cowl was in the same position. These particular runs were chosen because they show the full spectrum of the runs as 266 is at the furtherest forward point, 269 is furtherest back and 268 is in the middle. The cowl in the dynamic test is able to be lined up with the static locations accurately because the distances on the images can be scaled with respect to the top edge of the cowl as it is known.

The comparisons of runs 268 and 269 can be seen in Figures 5.3 and 5.4. It is obvious in figure 5.3 the actuation of the cowl makes a large impact on the starting of the inlet. It is clear in the images that the inlet in run 271 is started and running quite smoothly with only a small portion of the boundary layer trying to separate while the cowl in run 268 at the exact same location is unstarted.

Figure 5.4 does not clearly show many differences between the two runs. The only difference that can be seen is that the boundary layer trying to separate right before the cowl is a little bit stronger in run 271. This is negligible because during the entire 269 run there are times when the boundary layer trying to separate is as large as run 271 shows.

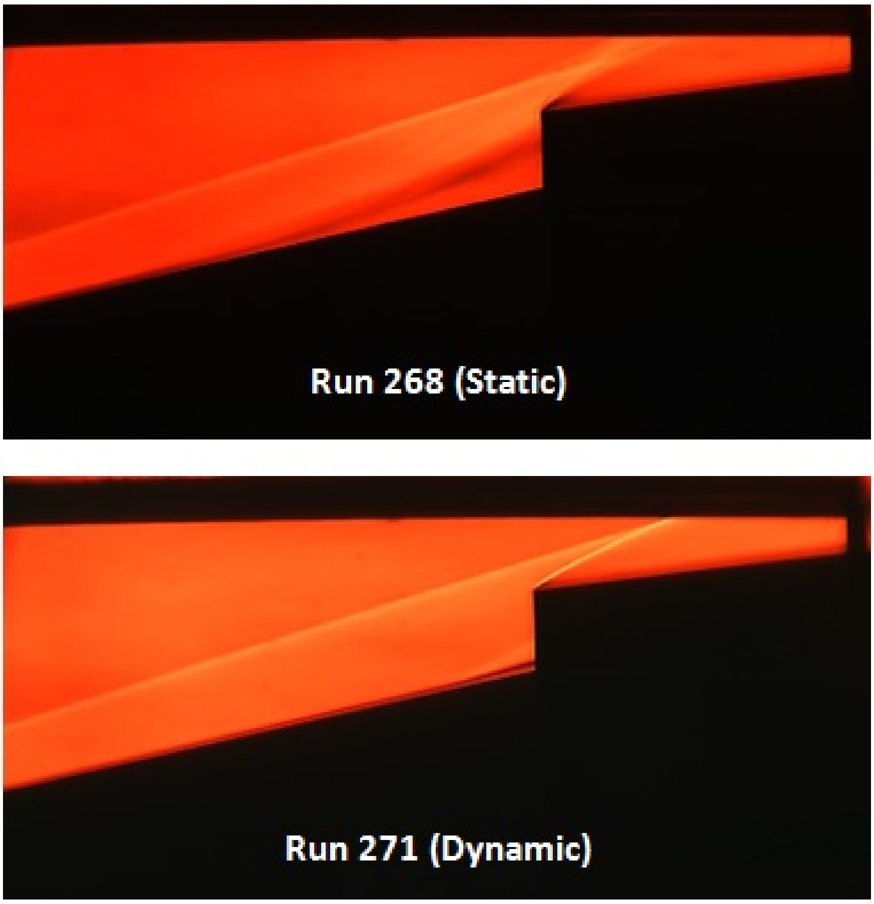

Figure 5.3: Comparison of run 268 and run 271 at the same position

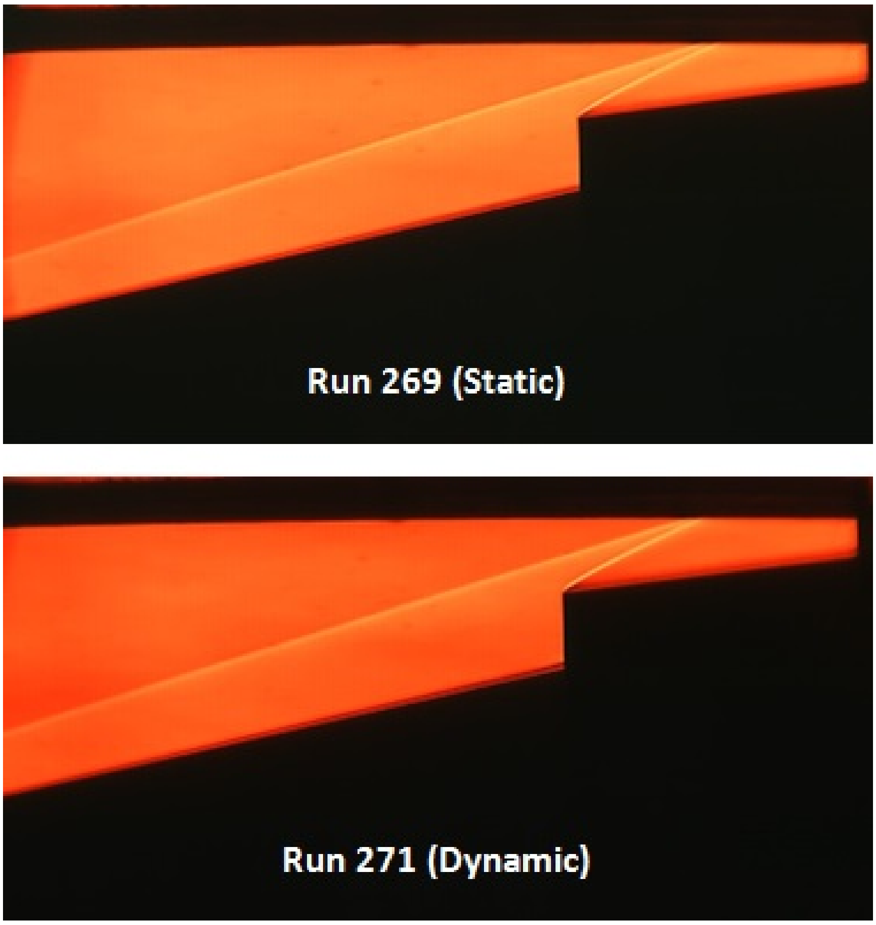

Figure 5.4: Comparison of run 269 and run 271 at the same position

The comparison of runs 266 and 271 was far more interesting because the rocking of the cowl had a large impact. Run 271 was setup so that the cowl would finish at the zero position and this is what allowed the rocking to affect the results. Figure 5.7 shows 1 ms before the collar hits the stop (top) and the 3 ms after in 1 ms intervals. As you can see the inlet in run 271 is started at the zero position, opposed to the unstarted static inlet in run 266 (Figure 5.5) at the zero position. Once the collar collides with the stopper in run 271 the inertia immediately starts to swing the leading edge of the cowl down and the impact of the collision also knocks the cowl and collar back a tiny distance. Even though the leading edge of the cowl is swinging down the inlet stays started until the last millisecond. However, as the edge swings down the boundary layer separation gets bigger each millisecond until its large enough to choke the inlet.

The pressure measurements indicate the same story as the flow visulisation. Figure 5.6 shows the surface pressure measurements for run 271. The length of time the cowl actuated was 17.5 ms as determined by analysis of the flow visulisation. Region A from figure 5.6 depicts the actuation time. It can be seen that during this time pressures 1

Figure 5.5: Flow visulisation of run 266

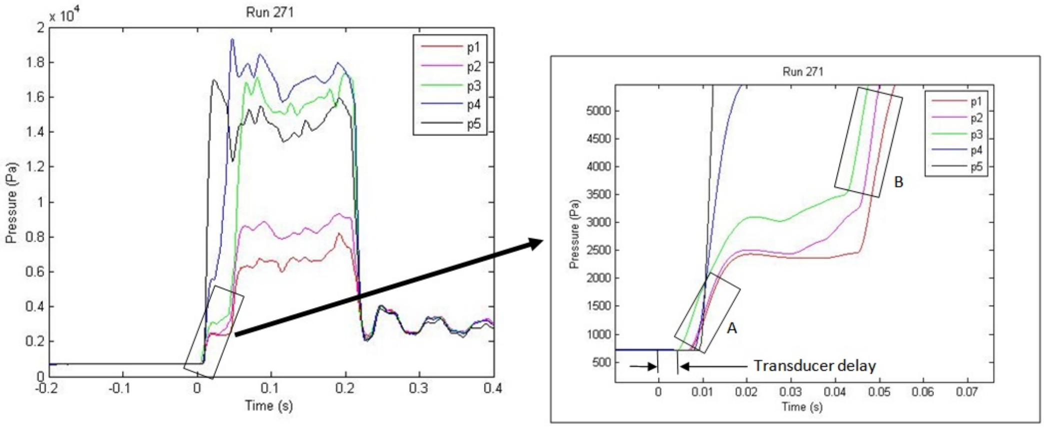

Figure 5.6: Surface pressure measurements of run 271

and 2 and almost identical and pressure 3 is a little bit larger but still follows the same pattern. This is caused by the boundary layer trying to separate near transducer 3, as seen in the flow visulisation. After the initial actuation period the pressures disperse for approximately 25 ms and then come close to combining again (region B) as the inlet tries to restart. This can also be seen in the flow visulisation but it is clear in the images that the attempt to restart doesn't last very long.

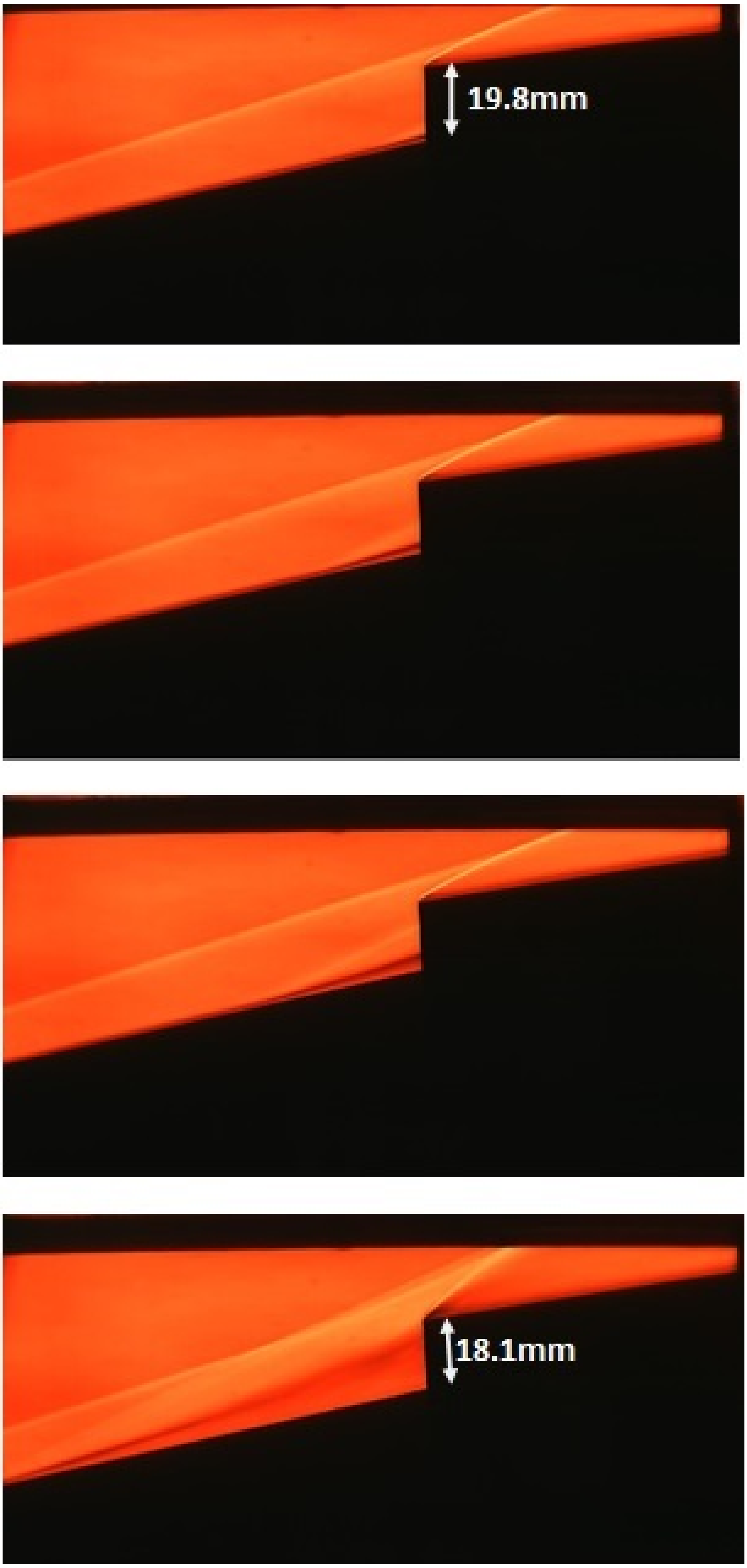

Figure 5.7: 1 ms before the end of actuation (top) followed by three images taken 1 ms apart after collision with stopper

Chapter 6

Conclusions

This project has designed a method of mounting and actuating the cowl on a axisymmetric scramjet inlet. The inlet was tested in Mach 6 conditions at the TUSQ facility under both static and dynamic cowl conditions. This chapter summaries the outcomes and conclusions regarding this work and discusses recommendations for future work.

6.1 Limitations

The main limitation encountered during this project was the way in which the cowl was found to rock backwards and forwards from the drag force. This rocking caused the ratio of contraction to continuously change throughout the test, which obviously affects the test results. After investigation, the reason for the rocking motion was a combination of; Clearances being to large between the collar and shaft, movement in the assembly joints and the deflection in the mount brackets caused by the drag forces acting on the cowl.

A smaller limitation which had less of an impact on the project was again to do with motion in the cowl. Instead of rocking backwards and forwards it also rolled a small amount side to side. The rolling motion existed because the mount brackets didn't run flush with the underside of the inlet body.

6.2 Static Tests

The unexpected rocking of the cowl makes it unrealistic to define definite static cowl positions where it starts and does not start. It is however, realistic to use the experimental results as an estimate of how the inlet behaves at each particular location. As expected, the static test runs done from the Kantrowitz limit backwards all resulted in an apparent started inlet, whereas, all tests done forward of the Kantrowitz limit resulted in an apparent unstarted inlet.

If time persisted, it would have been of value to further test the boundaries of the Kantrowitz limit as the closest test on the unstarted side was done 2.9 mm away. This would further help distinguish the working limits of the inlet. However, the experiments would prove to be relatively worthless if the issues with the rocking motion of the cowl were not addressed.

6.3 Dynamic Tests

The dynamic test worked very well and proved that the inlet could be in a started state where statically it would not have been started. The results showed that the actuated cowl was able to be started in every position that was statically tested (started and unstarted). This proves that dynamic actuation of the cowl could potentially be used to restart and unstarted inlet in flight.

If time enabled, it would have been beneficial to investigate the behaviour of the actuating cowl further forward than the 'zero' position. There is more than enough room in the actuation design for further movement and this could make it clear just how much further the cowl could go without unstarting.

6.4 Further Work

During the course of this project there have been a few questions left unanswered which could be answered with further investigations. Further work that could be investigated as a result of the work done in this project could include:

- Improving the guidance and actuation design by tightening the fit between the collar and shaft and also re-designing the mount brackets to eliminate deflection.
- Investigate further more definite boundaries and limitations of the static cowl conditions.
- Investigate the effect the actuating cowl would have along further distances and at different speeds.

6.5 Conclusion

In conclusion, this work involved the design and experimental testing of a system that can actuate a scramjet cowl during a test run. The results have shown that an actuating cowl, or potentially inlet body, can cause a scramjet inlet to start where it will not start under static cowl conditions.

References

ADFA (2007), *Scramjet Fuels Hydrogen Vs Hydrocarbon*, Fact Sheet, University of New South Wales & Australian Defence Force Academy. seit.unsw.adfa.edu.au/ojs/index.php/Hypersonics/article/view/18/8 [Online; accessed 11th May-2013].

AernauticalHandbook (2009), *Airplane Shock Waves*, Aeronautical Handbook, http://ma3naido.blogspot.com.au/2009/11/airplane-shock-waves.html. [Online; accessed 27th May-2013].

Andreadis, D. (2004), *Scramjets Integrate Air and Space*, Media Release, The Industrial Physicist. http://www.aip.org/tip/INPHFA/vol-10/iss-4/p24.html [Online; accessed 12th May-2013].

Beer, F. (2009), *Mechanics of Materials*, McGraw Hill, Ed. 5. Singapore.

Blau, P. (1992), 'Appendix: Static and kinetic friction coefficients for selected materials', *Friction, Lubrication and Wear Technology* **Vol 18**, pg 70–75. ASM Handbook.

Buttsworth, D. (2009), 'Ludwieg tunnel facility with free piston compression heating for supersonic and hypersonic testing', *Proceedings: Australian Space Science Conference* . September, Sydney.

Casper, K. (2009), 'Hypersonic wind-tunnel measurements of boundary-layer pressure fluctuations', *Proceedings:AIAA Fluid Dynamics Conference* . June, San Antonio, Texas.

Catalyst (2002), *Scramjet*, Television Story, ABC Australia. http://www.abc.net.au/catalyst/stories/s695744.htm.

CenterForHypersonics (2002), *HyShot Program Secures Place in Flight History*, University of Queensland, http://www.uq.edu.au/news/?article=3469. [Online; accessed 18th May-2013].

Covault, C. (2010), *X-51 Scramjet Flights Poised to Bridge Air and Space Propulsion for Space Launch, Prompt Global Strike*, Media Release, Spaceflight Now. http://spaceflightnow.com/news/n1005/16waverider/ [Online; accessed 20th May-2013].

Curran, E Murthy, S. (2000), 'Scramjet propulsion', *Progress in Astronautics and Aeronautics* **Vol 189**. AIAA American Institute of Aeronautics and Astronautics.

Fielding, S. (2007), 'Laminar boundary layer separation', *Department of Physics Durham University* .

FighterPlanes.com (2000), 'Military jet engines', http://engines.fighter-planes.com/jet_engine.htm. [Online; accessed 28th May-2013].

FIS (2007), 'What's a scramjet', http://www.456fis.org/WHAT'S_A_SCRAM_JET.htm. [Online; accessed 20th April-2013].

Fry, R. (2004), 'A century of ramjet propulsion technology evolution', *Journal of Propulsion and Power* **Vol 20**(No.1), pg 27–57. AIAA American Institute of Aeronautics and Astronautics.

Harrland, A. (2012), 'Hypersonic inlet for a laser powered propulsion system', *MPhil Dissertation, School of Engineering* . University of Adelaide.

Heiser, W Pratt, D. (1994), *Hypersonic Airbreathing Propulsion*, AIAA American Institute of Aeronautics and Astronautics. Washington, D.C.

Hibbeler, R. (2010), *Engineering Mechanics Dynamics*, Pearson, Ed. 12. Singapore.

HowThingsFly (2012), *Shock Waves*, Smithsonian National Air and Space Museum, http://howthingsfly.si.edu/aerodynamics/shock-waves. [Online; accessed 26th May-2013].

Hu, H. (2004), 'Flow visulization techniques: Shadowgraph and schlieren', *Department of Aerospace Engineering Iowa State University* .

Mahapatra, D. (2008), 'Shock tunnel studies on cowl/ramp shock interactions in a generic scramjet inlet', *Department of Aerospace Engineering* . Indian Institute of Science, Bangalore.

MathWorks (2013), 'Butterworth filter design', `http://www.mathworks.com.au/help/signal/ref/butter.html`. [Online; accessed October-2013].

Merriam-Webster (2010), 'Scramjet definition', `http://www.merriam-webster.com/dictionary/scramjet`. [Online; accessed May-2013].

NASA (2004), 'Astronomy picture of the day', `http://apod.nasa.gov/apod/ap040329.html`. [Online; accessed 28th May-2013].

NASA (2008), *Ramjet/Scramjet Thrust*, Fact Sheet, NASA. `http://www.grc.nasa.gov/WWW/k-12/airplane/ramth.html` [Online; accessed 25th May-2013].

NASA (2009*a*), *NASA Hyper-X Program Demonstrates Scramjet Technologies*, NASA Langley Research Centre, Hampton VA USA. `http://www.nasa.gov/centers/dryden/news/FactSheets/FS-040-DFRC.html`.

NASA (2009*b*), 'Nasa images - flow visulisation at mach 2', `http://archive.org/details/C-1955-37520`. [Online; accessed 2nd August-2013].

NASA (2009*c*), 'Schlieren system', `http://www.grc.nasa.gov/WWW/k-12/airplane/tunvschlrn.html`. [Online; accessed 23rd October-2013].

Prakash, D. (2006), 'Hypersonic intake studies', *M Tech Dissertation, Department of Aerospace Engineering* . Indian Institute of Technology, Bombay.

Pritchard, P. (2011), *Fox and McDonald's Introduction to Fluid Mechanics*, John Wiley & Sons, Ed. 8. USA.

Roberts, K. (2008), *Analysis and Design of a Hypersonic Scramjet Engine with a Starting Mach Number of 4.00*, University of Texas Arlington.

Smart, M. (2003*a*), *Scramjet Inlets*, Fact Sheet, Center for Hypersonics UQ. [Online; accessed 15th May-2013].

Smart, M. (2003*b*), *Scramjet Isolators*, Fact Sheet, Center for Hypersonics UQ. [Online; accessed 15th May-2013].

StandardsAustralia (1986), 'Fluid power - o-rings and housings - inch series, metric conversion', *Standards Australia* pp. AS 2842–1986. NSW.

Throckmorton, R., Schetz, J. & Jacobsen, L. (2010), *Experimental and Computational Investigation of a Dynamic Starting Method for Supersonic/Hypersonic Inlets*, Research Paper, AIAA American Institute of Aeronautics and Astronautics.

Wall, M. (2013), *Air Force's X-51A Hypersonic Scramjet Makes Record Breaking Final Flight*, Media Release, Space.com. `http://www.space.com/20967-air-force-x-51a-hypersonic-scramjet.html` [Online; accessed 25th May-2013].

Appendix A

Project Specification

<u>**ENG 4111/ ENG 4112 Research Project**</u>

PROJECT SPECIFICATION

FOR: Mitchell Kerr

TOPIC: Axisymmetric scramjet inlet operation with varying cowl positions

SUPERVISOR: David Buttsworth

PROJECT AIM: This project aims to investigate the operation of a scramjet inlet with varying axial positions of the cowl. A method of actuating the cowl will be designed so that the performance of the scramjet inlet can be quantified under static and dynamic cowl actuation conditions.

PROGRAMME:

1. Research the background information and analytical tools and techniques relating to conical scramjet design and cowl positioning

2. Design and develop a method of positioning and actuating the cowl.

3. Improve the mounting of the pressure transducers on the scramjet inlet.

4. Design an experiment to evaluate the performance of the inlet at different cowl positions. A number of appropriate static cowl positions will be targeted, along with a smaller number of conditions which target dynamic cowl operation.

5. Analyse the performance of the inlet in the hypersonic wind tunnel via pressure transducer measurements and schlieren flow visualisation.

6. Assess experimental results within the context of the analytical tools and techniques for inlet design and cowl positioning.

Appendix B

Manufacturing Drawings

PRODUCED BY AN AUTODESK EDUCATIONAL PRODUCT

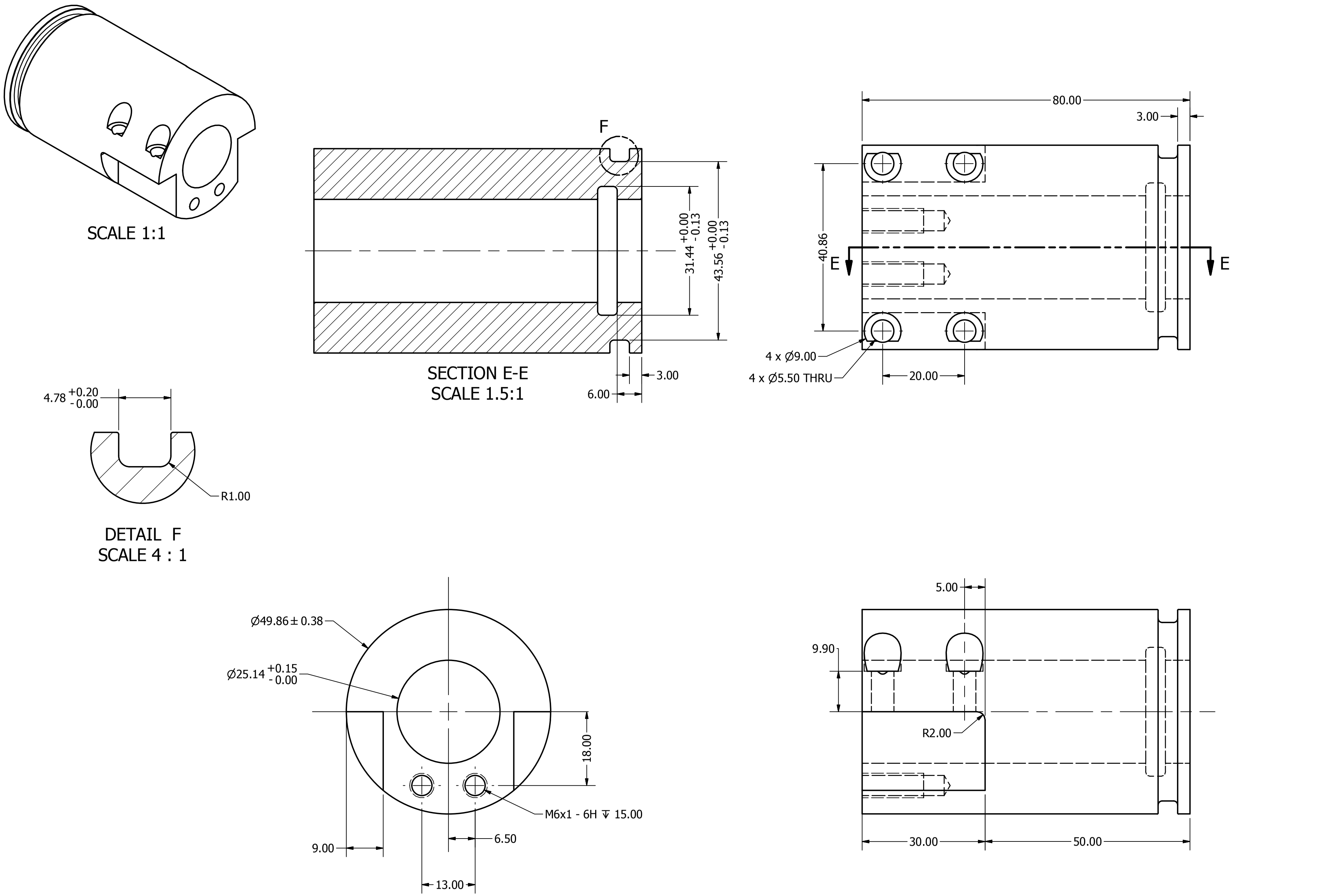

NOTE: O-RING SIZE NUMBERS 210 x 1 AND 225 x 1 REQUIRED

MILD STEEL	
TITLE	COLLAR
SIZE	C
DWG NO	
REV	
SCALE	
SHEET	2 OF 8

PRODUCED BY AN AUTODESK EDUCATIONAL PRODUCT
PRODUCED BY AN AUTODESK EDUCATIONAL PRODUCT
PRODUCED BY AN AUTODESK EDUCATIONAL PRODUCT

PRODUCED BY AN AUTODESK EDUCATIONAL PRODUCT

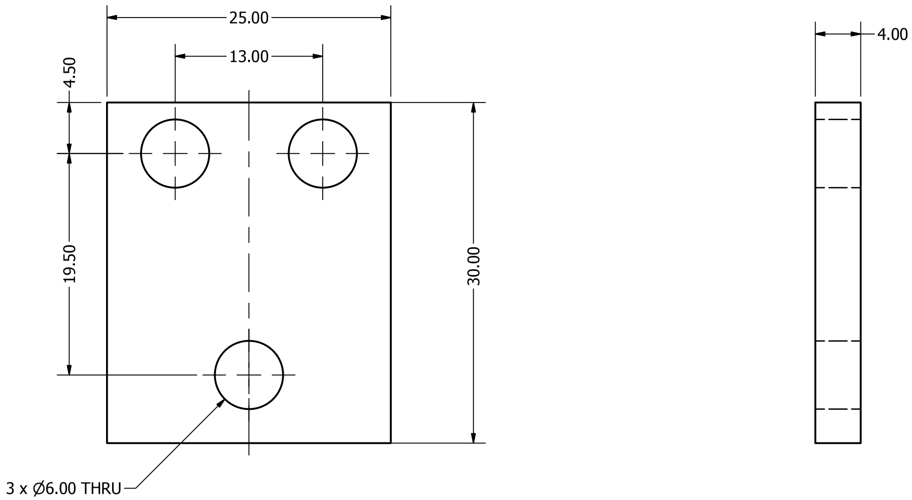

MILD STEEL	
TITLE GUIDE PLATE	
SIZE C	DWG NO	REV
SCALE	SHEET 3 OF 8

PRODUCED BY AN AUTODESK EDUCATIONAL PRODUCT
PRODUCED BY AN AUTODESK EDUCATIONAL PRODUCT
PRODUCED BY AN AUTODESK EDUCATIONAL PRODUCT

PRODUCED BY AN AUTODESK EDUCATIONAL PRODUCT

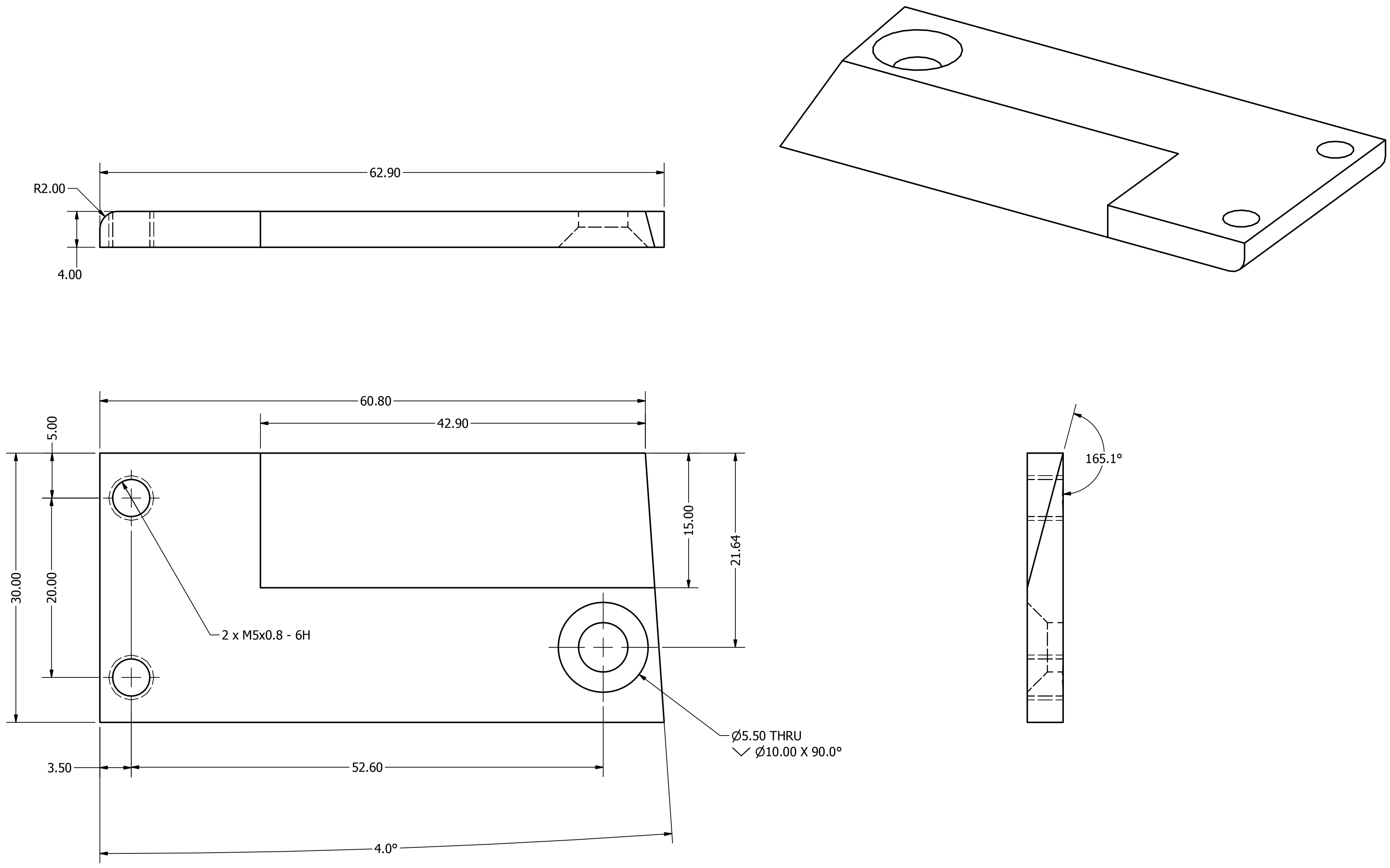

MILD STEEL			
TITLE LEFT MOUNT BRACKET			
SIZE C		DWG NO	REV
SCALE		SHEET 4 OF 8	

PRODUCED BY AN AUTODESK EDUCATIONAL PRODUCT
PRODUCED BY AN AUTODESK EDUCATIONAL PRODUCT
PRODUCED BY AN AUTODESK EDUCATIONAL PRODUCT

PRODUCED BY AN AUTODESK EDUCATIONAL PRODUCT

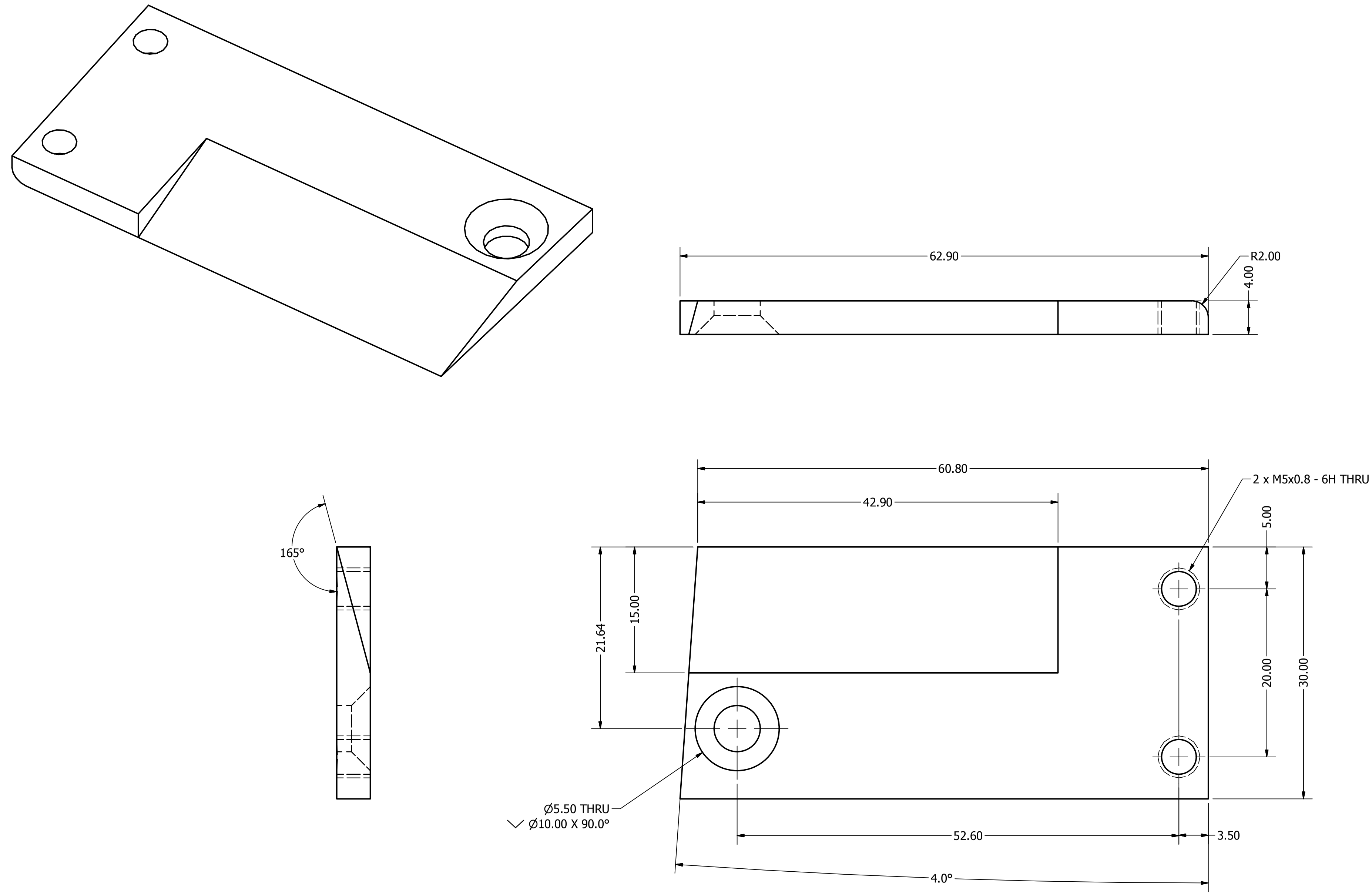

MILD STEEL		
TITLE RIGHT MOUNT BRACKET		
SIZE C	DWG NO	REV
SCALE		SHEET 5 OF 8

PRODUCED BY AN AUTODESK EDUCATIONAL PRODUCT
PRODUCED BY AN AUTODESK EDUCATIONAL PRODUCT

PRODUCED BY AN AUTODESK EDUCATIONAL PRODUCT

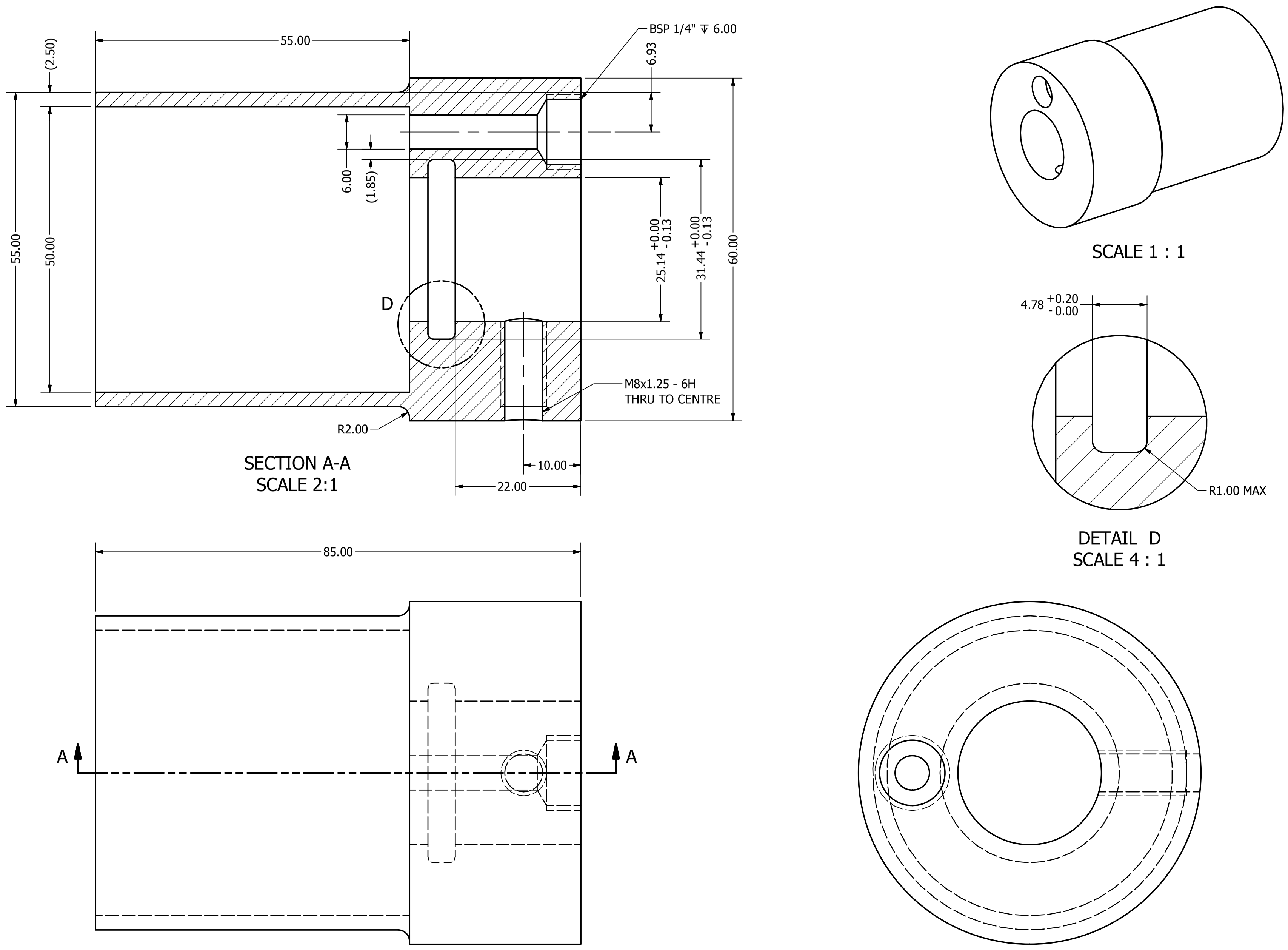

NOTE: O-RING SIZE NUMBER 210 x 1 REQUIRED

MILD STEEL	
TITLE: PRESSURE FITTING	
SIZE: C	DWG NO	REV
SCALE	SHEET 6 OF 8

PRODUCED BY AN AUTODESK EDUCATIONAL PRODUCT
PRODUCED BY AN AUTODESK EDUCATIONAL PRODUCT

PRODUCED BY AN AUTODESK EDUCATIONAL PRODUCT

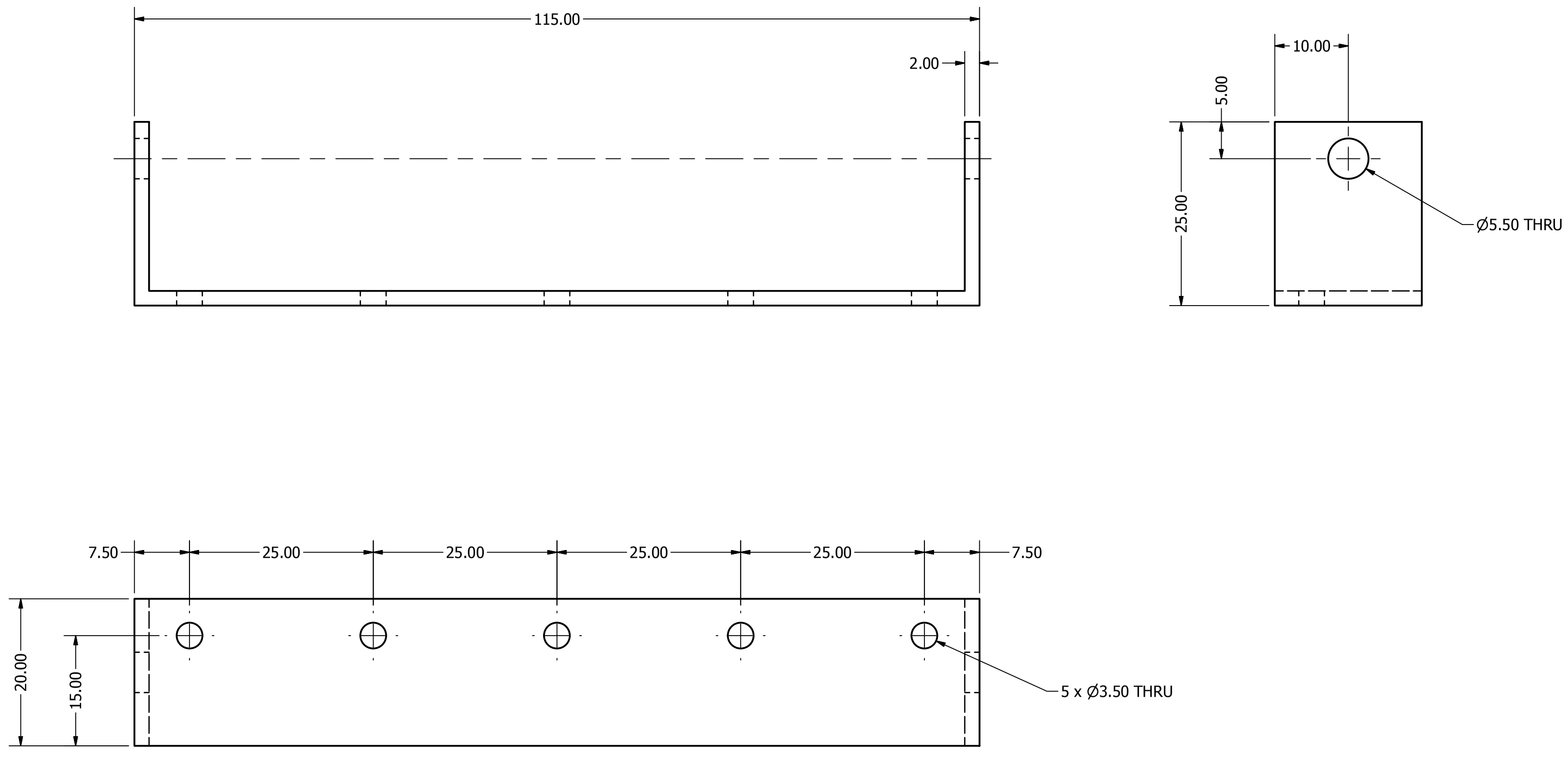

ALUMINUM

TITLE
TRANSDUCER MOUNT

SIZE C | DWG NO | REV

SCALE | SHEET 7 OF 8

PRODUCED BY AN AUTODESK EDUCATIONAL PRODUCT
PRODUCED BY AN AUTODESK EDUCATIONAL PRODUCT
PRODUCED BY AN AUTODESK EDUCATIONAL PRODUCT

PRODUCED BY AN AUTODESK EDUCATIONAL PRODUCT

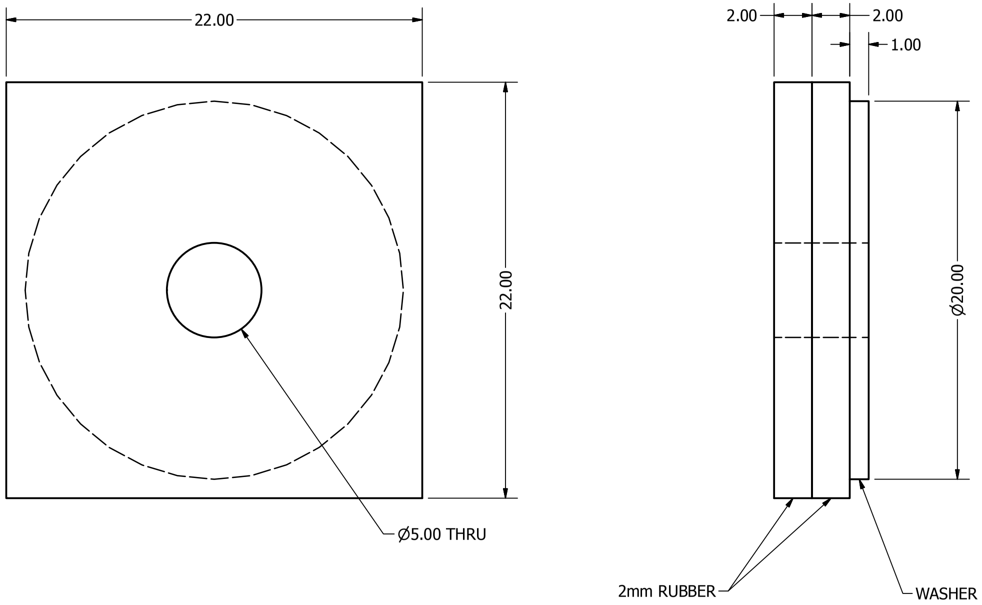

NOTE: ITEMS GLUED TOGETHER

TITLE	STOP	
SIZE C	DWG NO	REV
SCALE		SHEET 8 OF 8

PRODUCED BY AN AUTODESK EDUCATIONAL PRODUCT

Appendix C

Matlab Code

C.1 The `kantrowitzlimit.m` MATLAB Script

Listing C.1: Code to Calculate Kantrowitz Limit

```
% Kantrowitz Limit Calculation
% Axi-symmetric Scramjet Inlet

clear
clc

increment=1;     % Simulation increment
cowlL=71.6;      % Length of cowl

% Range in x direction
x=[0:increment:cowlL];

% Slope representing inlet
y1= -0.2177*x+62.2;

% slope representing inside surface of cowl
y2=sqrt(1104.1^2-(x-179.919).^2)-1023.795;

% Represents poistion at throat of inlet
for i=[1:((cowlL/increment)+1)]
    y3(1:i)=62.2;
end

% Plot geometry
figure (1)
plot(x,y1,'-.');
hold on
plot(x,y2,'--');
hold on
plot(x,y3)
legend('Inlet','Cowl','Inlet Throat Position')
xlabel('Distance From Throat (mm)')
ylabel('Distance From Axis (mm)')
title('Representation of Inlet Geometry')

% Position where lip of cowl is
Pos=(length(x)-(x/increment));

% Simulating moving cowl back
for q = 1:length(x) % Area at location 2
    a2(1,q)= (pi*y2(length(y2)).^2)-(pi*(y1(Pos(q)).^2));
end

% Throat area
at=(pi*y2.^2)-(pi*y3.^2);

% Area required to suit Kantrowitz Limit
a2req= 1.572*at;
```

```
% Difference between Area 2 actual and required
p=a2-a2req;

% Magnitute of errors so minimum can be found
r=abs(p);

% Mimimum error
KP=min(r);

 % Find where Minimum error is located (Kantrowitz Limit
    location)
 % Measured distance from throat
Kantr_C_Lip_Pos = find(r==KP)

% Shows amount of error from the limit for each position
figure (2)
plot(x,p)
hold on
plot(x,r)
xlabel('Distance From Throat (mm)')
ylabel('Difference between Actual Area 2 and Area 2 to Suit
   Kantrowitz Limit')
title('Error From Kantrowitz Limit at Each Position')
```

C.2 The MachNo.m MATLAB Script

Listing C.2: Code to Calculate Flow Conditions

```
% Find Mach number, Temperature, Speed of Sounds & Velocity
% Based on isentropic equations
clear
clc

% Pressures
Po =
    [920800,926800,927600,931700,920000,1000000,919500,946300];
Pe = [810,790,640,670,720,800,710,710];

%ratio of specific heats
k = 1.4;

% Mach numner
for i = 1:length(Po)
    Me(1,i) = sqrt((((Po(i)/Pe(i))^(1/(k/(k-1))))-1)/((k-1)/2)
        );
end

% Temperature of flow
T0 = 560 ;
for i = 1:length(Po)
    T(1,i) = T0/(1+((k-1)/2)*Me(i)^2);
end

% Speed of sound
R = 287; %N.m/(kg.K) for air

for i = 1:length(Po)
    c(i) = sqrt(k*R*T(i));
end

% Velocity of flow
for i = 1:length(Po)
    V(i) = Me(i)*c(i);
end

% Output to command window
Me
T
c
V
```

Appendix D

Pressure Results

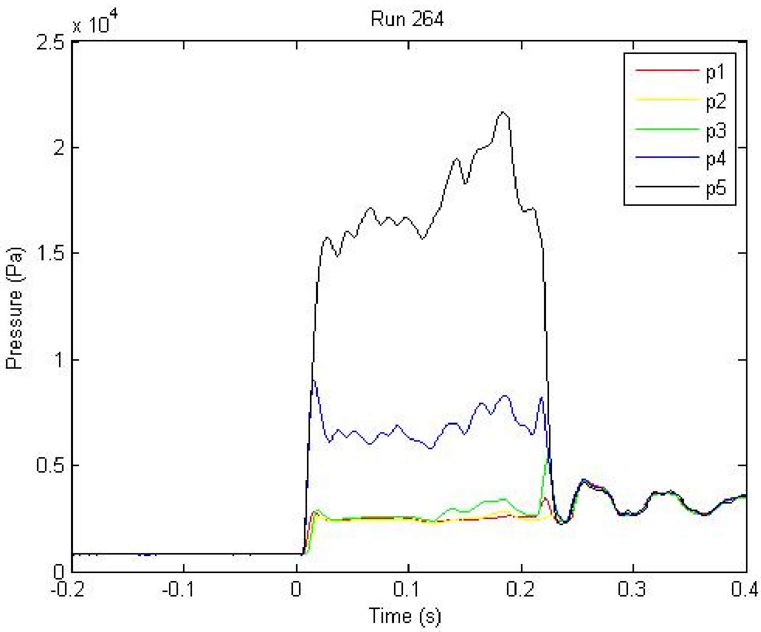

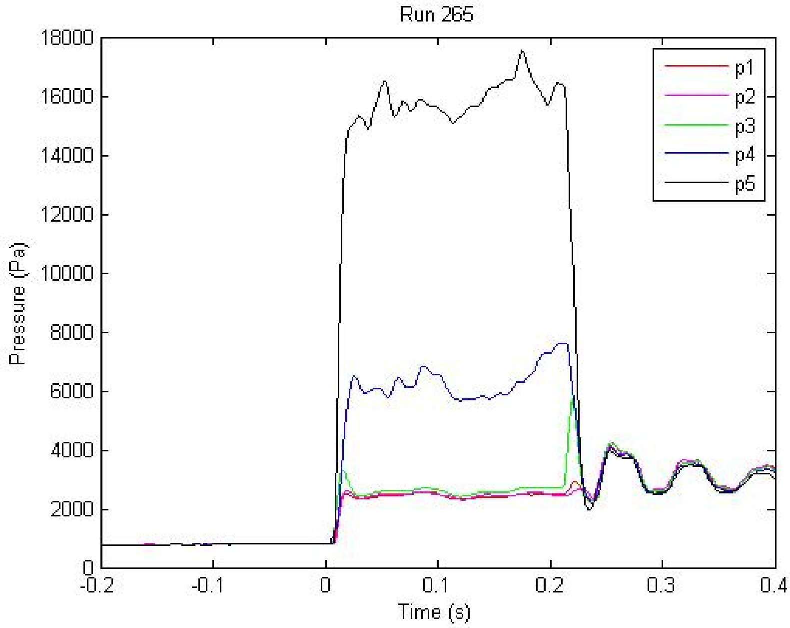
Run 265
18000
16000
14000
12000
10000
8000
6000
4000
2000
0
-0.2
-0.1
0
0.1
0.2
0.3
0.4
Time (s)
Pressure (Pa)
p1
p2
p3
p4
p5

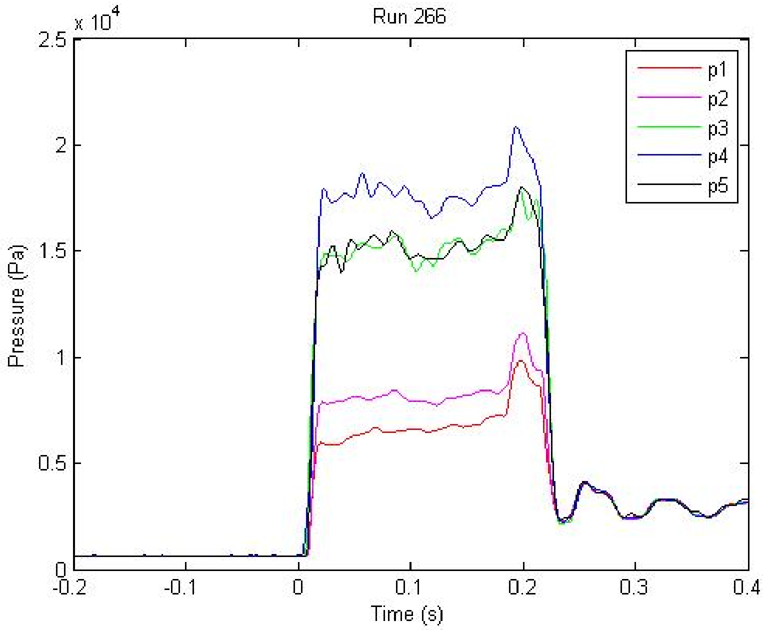
Run 266
x 10^4
2.5
2
1.5
1
0.5
0
-0.2
-0.1
0
0.1
0.2
0.3
0.4
Time (s)
Pressure (Pa)
p1
p2
p3
p4
p5

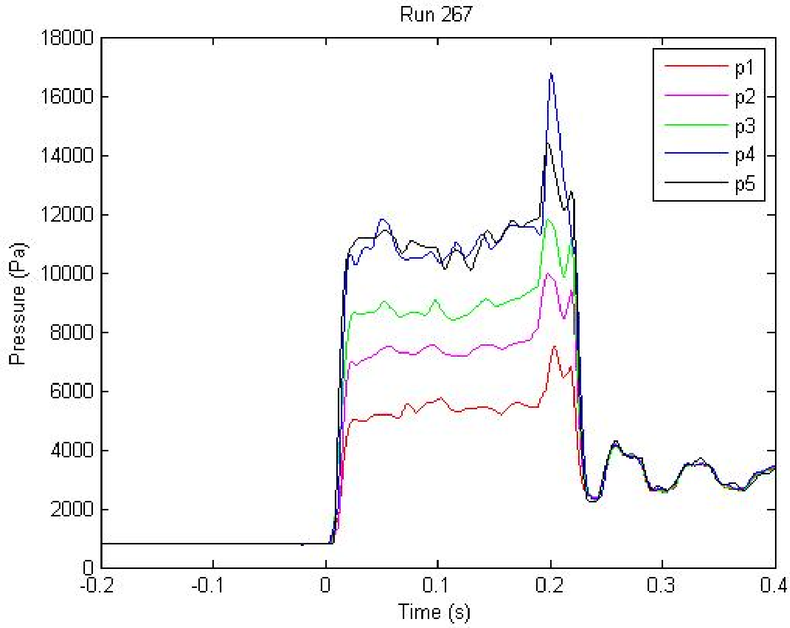

Run 267
Pressure (Pa)
Time (s)
p1
p2
p3
p4
p5
0
2000
4000
6000
8000
10000
12000
14000
16000
18000
-0.2
-0.1
0
0.1
0.2
0.3
0.4

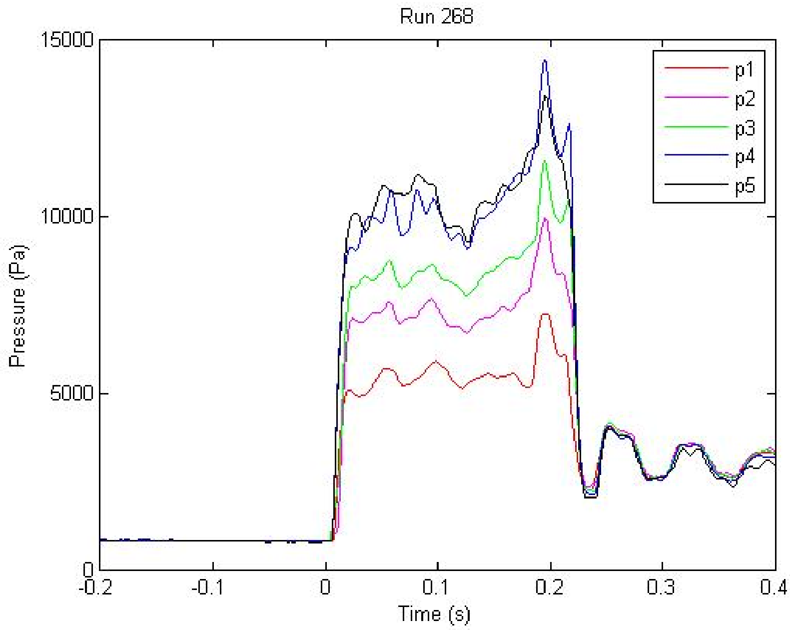

Run 268
Pressure (Pa)
Time (s)
p1
p2
p3
p4
p5
0
5000
10000
15000
-0.2
-0.1
0
0.1
0.2
0.3
0.4

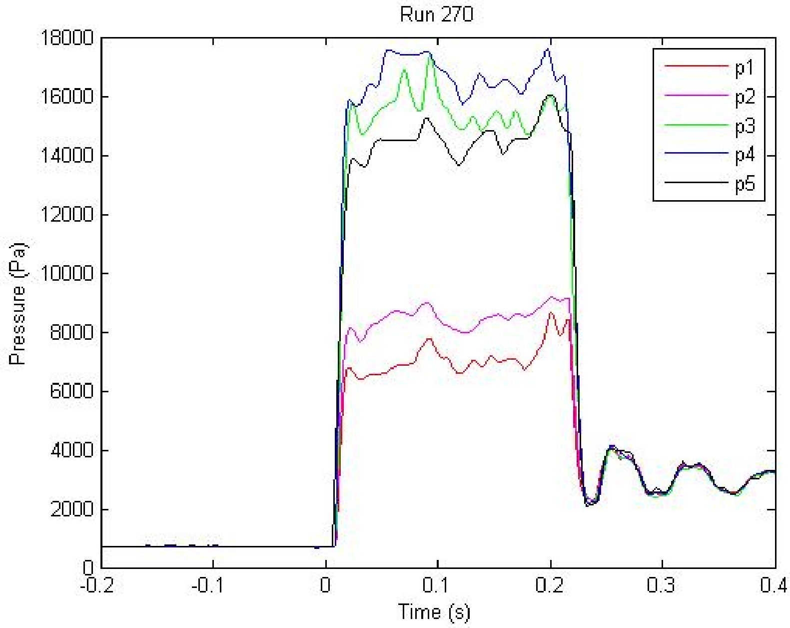
Run 270
Pressure (Pa)
Time (s)
p1
p2
p3
p4
p5
18000
16000
14000
12000
10000
8000
6000
4000
2000
0
-0.2
-0.1
0
0.1
0.2
0.3
0.4

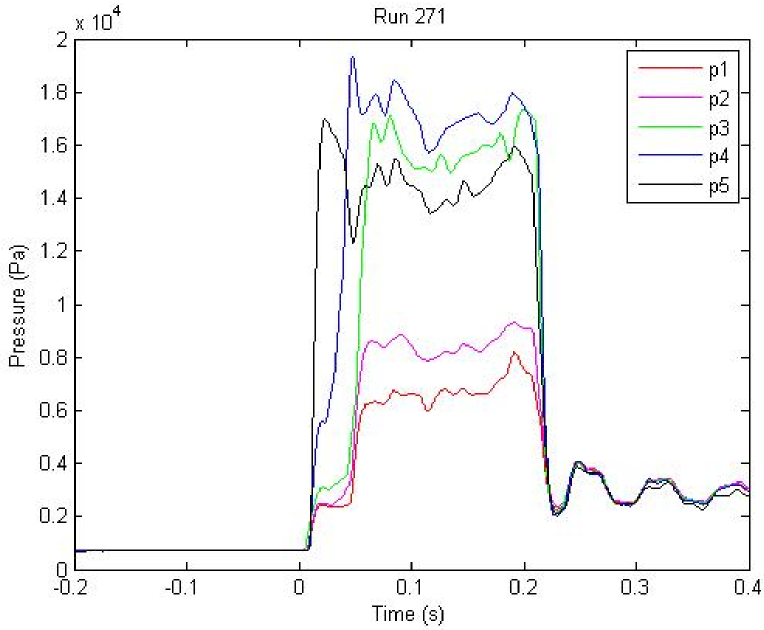
Run 271
x 10^4
Pressure (Pa)
Time (s)
p1
p2
p3
p4
p5
2
1.8
1.6
1.4
1.2
1
0.8
0.6
0.4
0.2
0
-0.2
-0.1
0
0.1
0.2
0.3
0.4

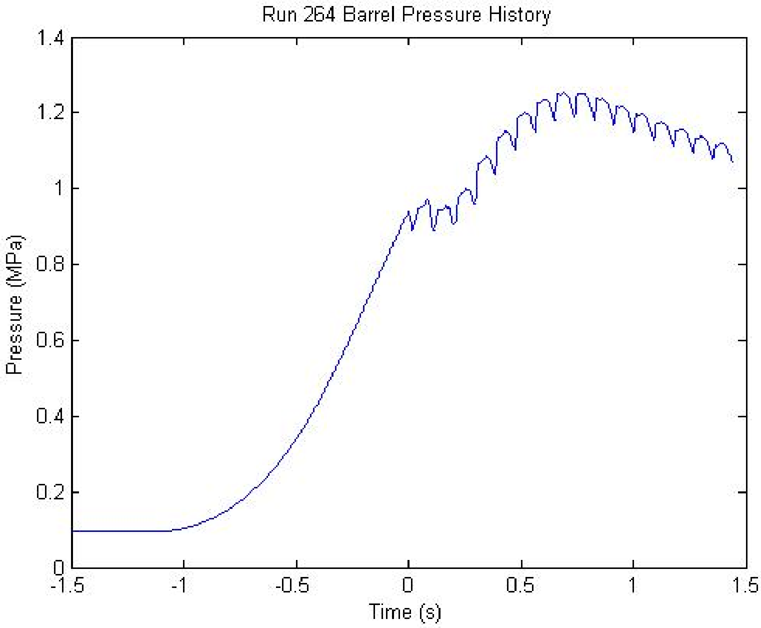
Run 264 Barrel Pressure History
Pressure (MPa)
Time (s)
1.4
1.2
1
0.8
0.6
0.4
0.2
0
-1.5
-1
-0.5
0
0.5
1
1.5

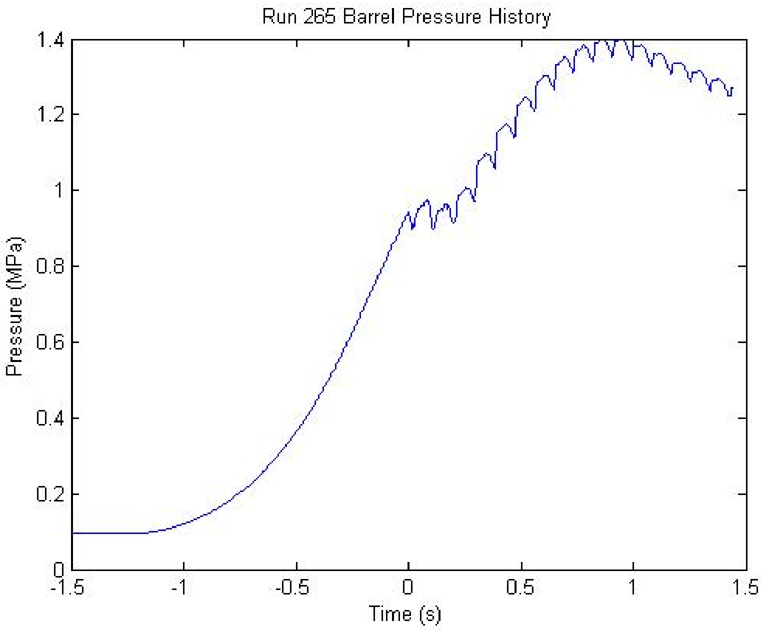
Run 265 Barrel Pressure History
Pressure (MPa)
Time (s)
1.4
1.2
1
0.8
0.6
0.4
0.2
0
-1.5
-1
-0.5
0
0.5
1
1.5

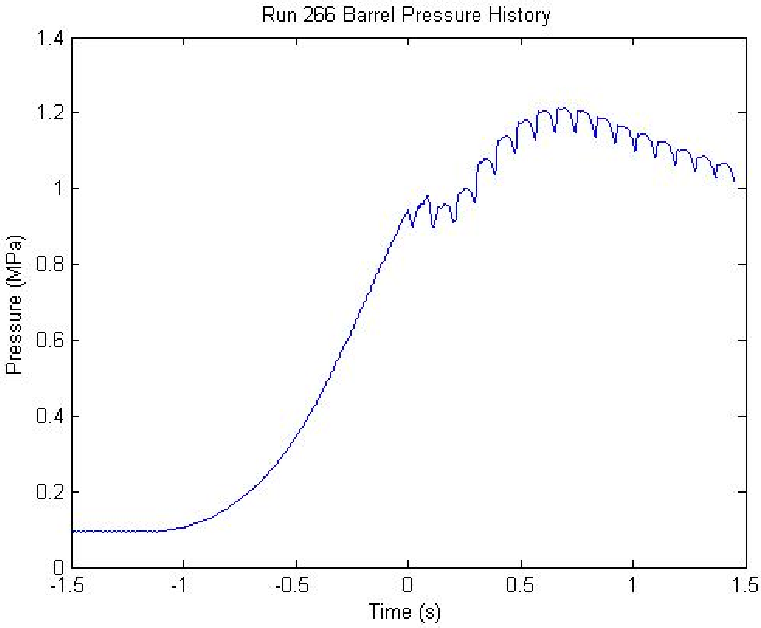
Run 266 Barrel Pressure History
Pressure (MPa)
Time (s)
0
0.2
0.4
0.6
0.8
1
1.2
1.4
-1.5
-1
-0.5
0
0.5
1
1.5

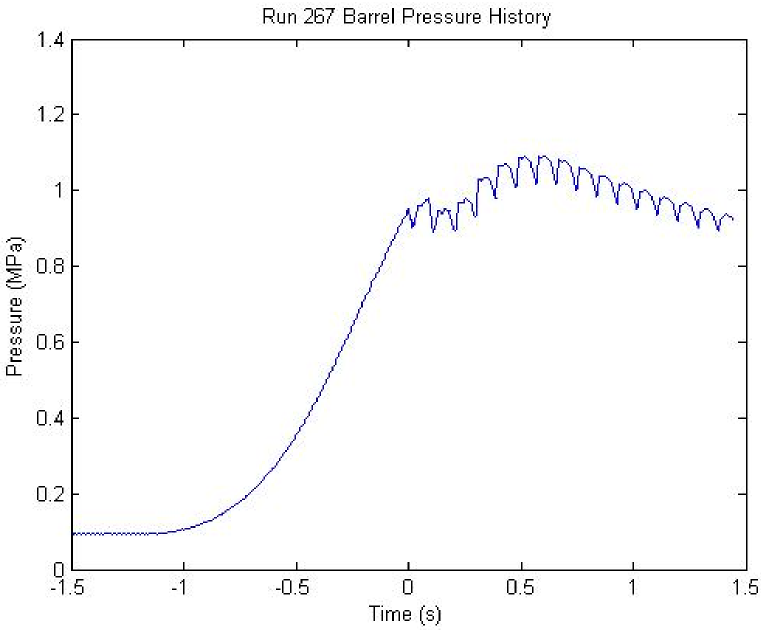
Run 267 Barrel Pressure History
Pressure (MPa)
Time (s)
0
0.2
0.4
0.6
0.8
1
1.2
1.4
-1.5
-1
-0.5
0
0.5
1
1.5

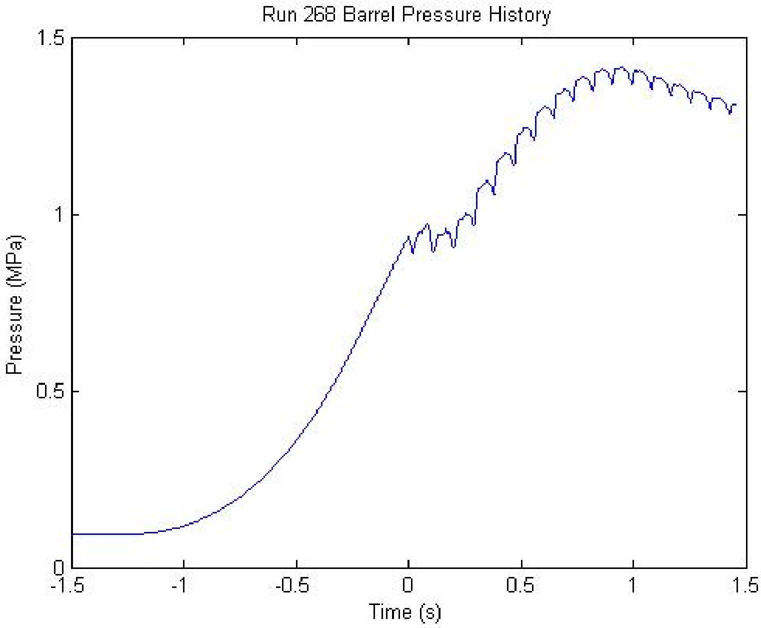
Run 268 Barrel Pressure History
Pressure (MPa)
Time (s)
1.5
1
0.5
0
-1.5
-1
-0.5
0
0.5
1
1.5

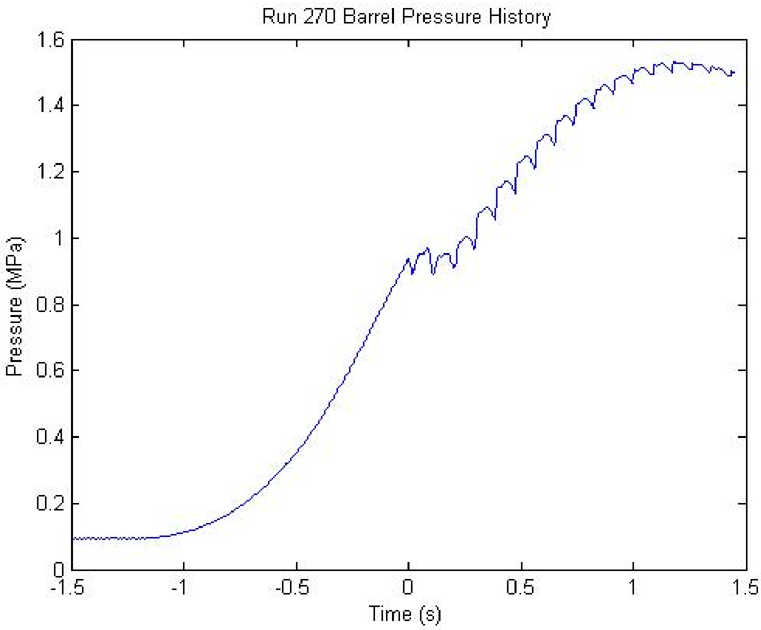
Run 270 Barrel Pressure History
Pressure (MPa)
Time (s)
1.6
1.4
1.2
1
0.8
0.6
0.4
0.2
0
-1.5
-1
-0.5
0
0.5
1
1.5

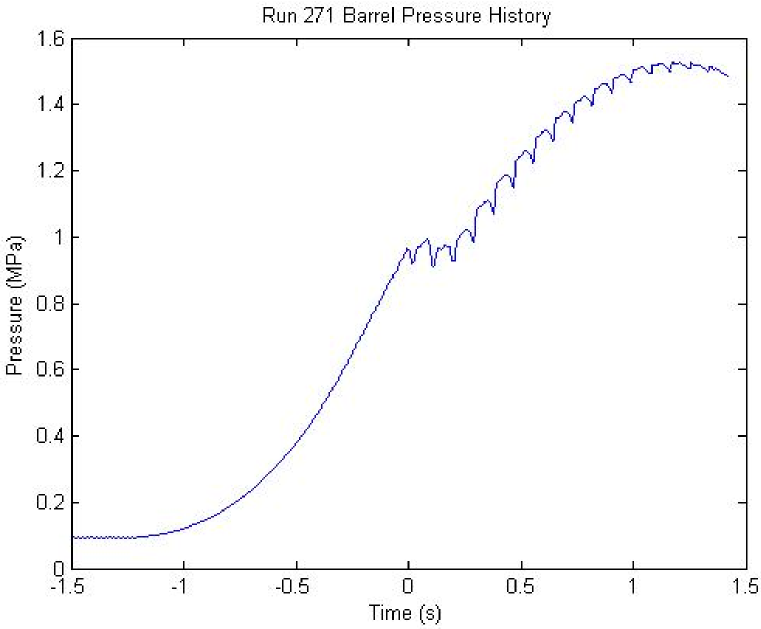
Run 271 Barrel Pressure History
Pressure (MPa)
Time (s)
1.6
1.4
1.2
1
0.8
0.6
0.4
0.2
0
-1.5
-1
-0.5
0
0.5
1
1.5